SUPERCRITICAL CARBON DIOXIDE EXTRACTION

A Thesis

presented to

the Faculty of California Polytechnic State University,

San Luis Obispo

In Partial Fulfillment

of the Requirements for the Degree

Master of Science in Mechanical Engineering

by

Kevin Carney

June 2017

COMMITTEE MEMBERSHIP

TITLE: Supercritical Carbon Dioxide Extraction

AUTHOR: Kevin Carney

DATE SUBMITTED: June 2017

COMMITTEE CHAIR: Steffen Peuker, Ph.D.
Professor of Mechanical Engineering

COMMITTEE MEMBER: Scott Patton, Ph.D.
Professor of Mechanical Engineering

COMMITTEE MEMBER: Jesse Maddren, Ph.D.
Professor of Mechanical Engineering

ABSTRACT

Supercritical Carbon Dioxide Extraction

Kevin Carney

The objective of this thesis is to explore the properties of supercritical carbon dioxide (CO_2) and the feasibility of building a small-scale low cost system. A supercritical fluid is a fluid which exhibits properties between liquid and gas with liquid like densities and viscosities similar to a gas. Since the discovery of supercritical fluids in 1822, the use of supercritical fluids, specifically supercritical CO_2, has grown in popularity. The application of supercritical CO_2 has continued to grow in industrial applications since the 1970's. Due to CO_2's many beneficial properties as a "green" solvent, supercritical CO_2 as a solvent is able to be implemented in a wide range of applications from aerospace, microchip manufacturing, food production, biomedical, pharmaceutical, dry-cleaning, and many more.

This thesis project included designing, building and testing a supercritical CO_2 extraction apparatus that examines the use of supercritical CO_2 as a solvent in the extraction process of decaffeinating coffee. Due to the fact that supercritical CO_2 requires high pressure operating conditions, the apparatus design is important not only for function but also for safety. In the description portion of this paper, design considerations related to each component's function and their specific roles in the overall system are clearly stated. Furthermore, the build process is outlined along with the overall step-by-step operation of the final system.

Different methods of data measurements are taken while the system is running in order to interpret the apparatus' overall functionality. Through the exploration of this

collected experimental data, the results were compared between different operating parameters. In order to determine the feasibility of the supercritical thesis apparatus, it was tested by applying the supercritical CO_2 as a solvent for the extraction of caffeine from coffee beans. Analysis of the analytical data recorded from experimental testing confirms that the apparatus produced supercritical CO_2. After testing specific operating conditions, it is proven that the supercritical CO_2 is able to function as a "green" solvent in this small-scale system. The experimental results from these analytical runs are compared with theoretical maximums in order to determine efficiency.

Lastly, the paper presents an overview including lessons learned from the design process and from the information gathered. Data from experimental testing is interpreted and the system design is reevaluated with suggestions for future improvements.

Keywords: Supercritical Carbon Dioxide Extraction, Green Solvent, Closed Loop System

TABLE OF CONTENTS

LIST OF TABLES

Table Page

LIST OF FIGURES

Figure Page

Chapter 1: Introduction

1.1 Supercritical CO_2

Supercritical, also known as transcritical, fluids change into a two-state phase (liquid-gas state) once they exceed their critical point pressure and temperature. A fluid is in a supercritical state when both the temperature and pressure exceed the fluids' unique critical point values (Mukhopadhayay, 2000). When gas is heated beyond a specific temperature where no amount of compression will cause it to become liquid this is known as the critical temperature and pressure. A supercritical fluid contains the properties of both gas and liquid beyond the critical point. In this thesis this state is referred to as supercritical.

In 1822 Baron Cagniard de la Tour observed the first reported occurrence of this supercritical phase (Taylor, 2000). In the late 1970's and early 1980s the boom of research and experimentation regarding the applications and properties of supercritical fluids began. Zosel's patent was a crucial development in the realization of supercritical fluid extraction and "provided incentive for extensive future work" due to the profitability of the patent (Taylor, 1996).

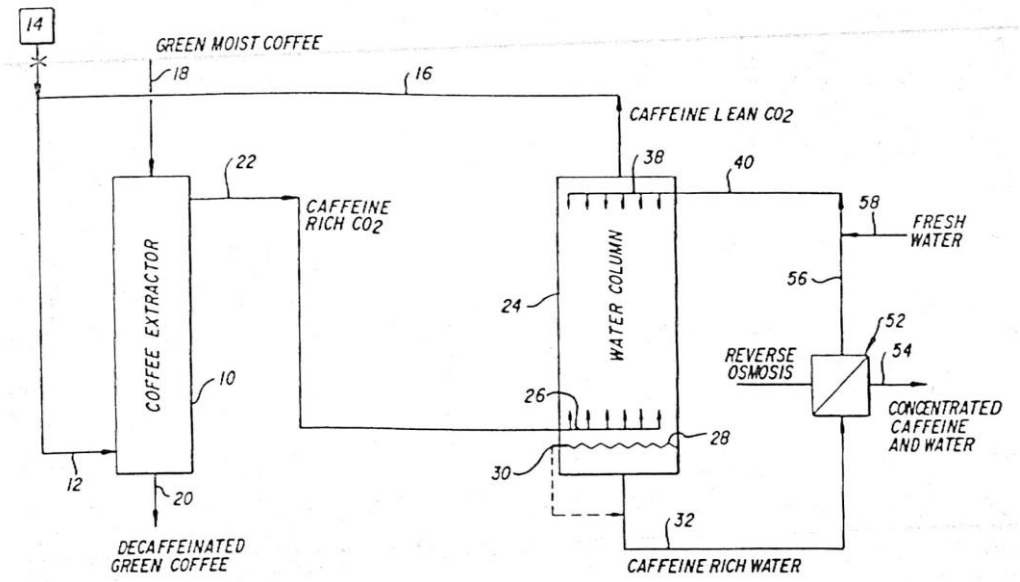

Figure 1: Schematic for Large Scale Coffee Decaffeination (McHugh, 1994)

Since this development, researchers have explored the multitude of applications of supercritical CO_2; currently these applications include: extraction of coffee and tea decaffeination, nicotine extraction, hops extraction, flavors extraction, cleaning of electronic and biomedical parts, color extraction, and aroma extraction (Taylor, 1996). Figure 1 shows the schematic for the large scale supercritical CO2 coffee decaffeination plant seen in Figure 2.

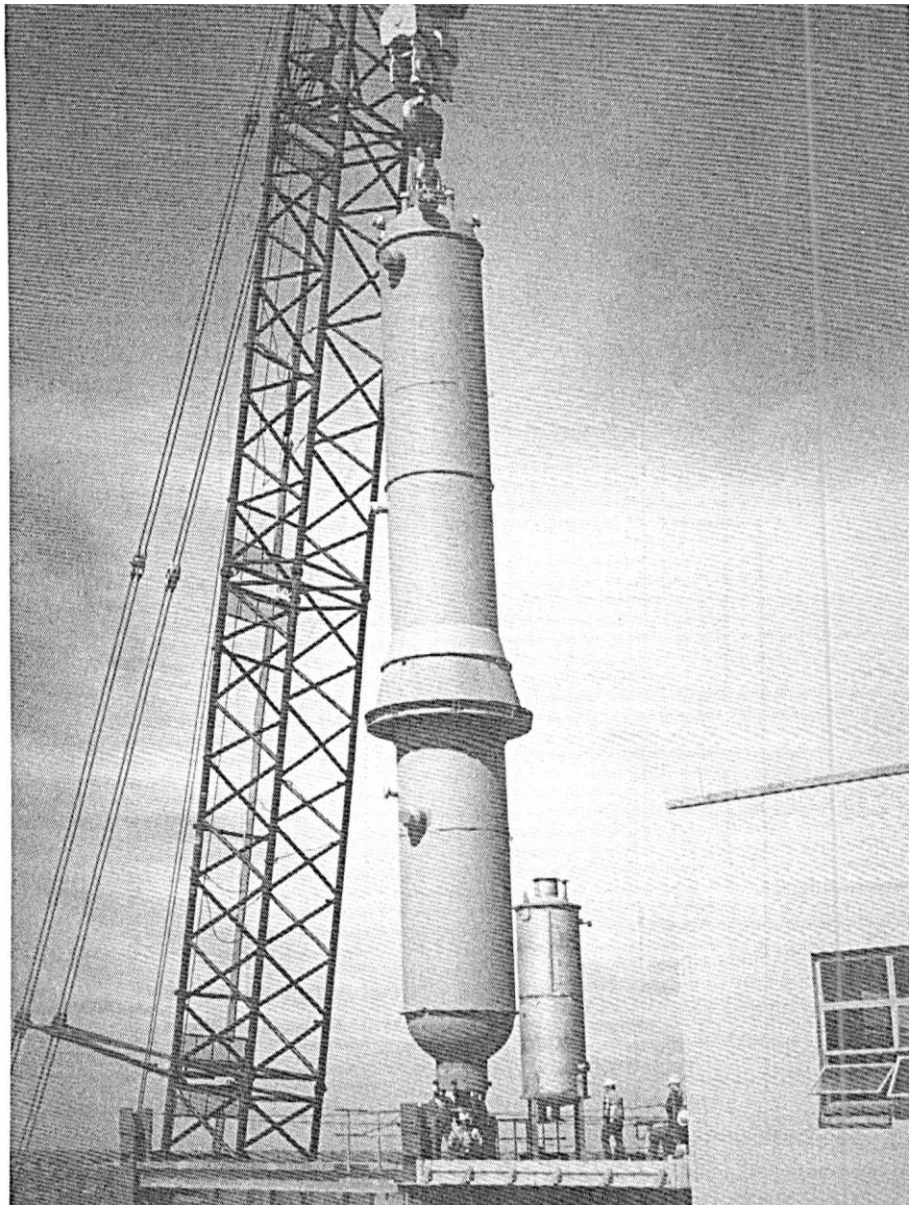

Figure 2: Industrial Supercritical CO_2 Extraction Vessel (McHugh, 1994)

Supercritical CO_2 offers appealing extraction properties due to its favorable viscosity, surface tension, diffusivity, and other physical properties. CO_2's critical point is 87.8°F while its critical pressure is 1073 psi. One of the most important factors in the research of this thesis is CO_2's critical point – i.e. the point at which vapor can no longer be distinguished from liquid (Taylor, 1996).

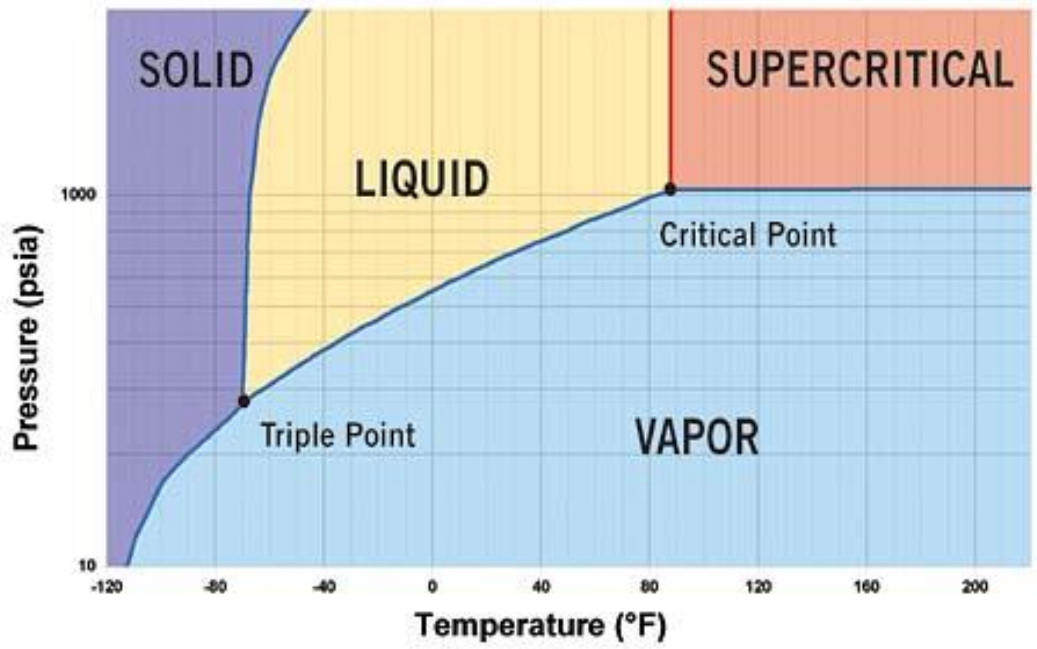

Figure 3: Phase Diagram for CO_2 (Source: http://www.gridgit.com)

Figure 3 shows the phase diagram for CO_2 with the areas corresponding states of the fluid labeled. The triple point can be seen in the bottom left hand corner where the Solid-Liquid-Vapor regions meet. The critical point, which is unique to supercritical fluids can be seen in the upper right of the graph and is where the Liquid-Vapor-Supercritical regions meet. Table 1 shows the unique pressure and temperature conditions at which a substance reaches its critical point for various supercritical solvents. Carbon Dioxide has lower pressure and temperature requirements than any of the other solvents, as seen in Table 1, in order to reach its critical point and become a supercritical fluid.

Table 1: Supercritical Fluids with corresponding Pressures (McHugh, 1994)

Solvent	Critical Temperature (°C)	Critical Pressure (MPa)
Carbon Dioxide	31.1	7.38
Ethane	32.2	4.88
Ethylene	9.3	5.04
Propane	96.7	4.25
Propylene	91.9	4.62
Cyclohexane	280.3	4.07
Isopropanol	235.2	4.76
Benzene	289	4.89
Toluene	318.6	4.11
p-Xylene	343.1	3.52
Chlorotrifluoromethane	29.8	3.92
Trichlorofluoromethane	198.1	4.41
Ammonia	132.5	11.28
Water	374.2	22.05

Once CO_2 reaches its critical point, CO_2 becomes a one-phase fluid where it has characteristics of both a liquid and a gas in the transcritical region. In its supercritical state CO_2's properties makes it suitable to be used as a solvent.

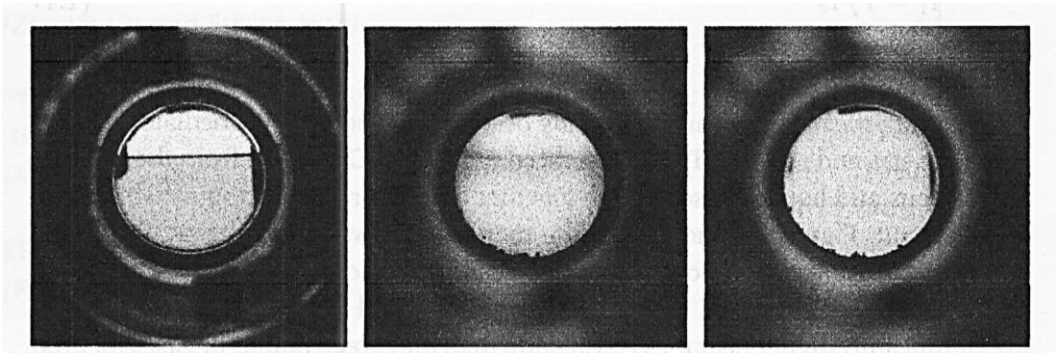

Figure 4: Transition from liquid CO_2 into Supercritical CO_2, heating in closed vessel (Leitner, 2010)

The strength of the supercritical fluid to act as a solvent is determined by the density of the fluid. The denser the supercritical fluid is the better it preforms as a solvent. This is why gases normally do not make good solvents compared with more common organic

solvents such as acetone, benzene, chloroform, ethanol, hexane, methanol, pentane or petroleum ether (McHugh, 1994).

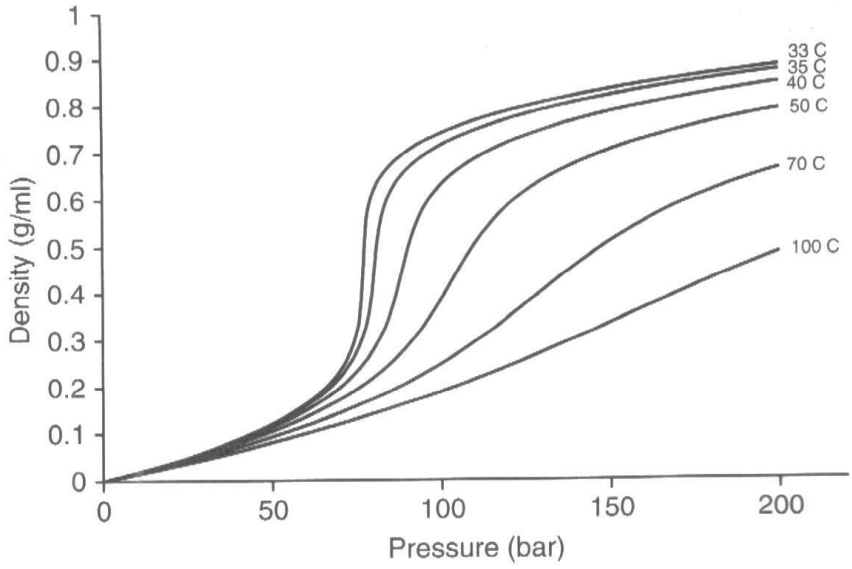

Figure 5: Supercritical CO_2 Plot Pressure vs. Density (Gupta, 2007)

Research into supercritical CO_2 is being conducted because it is a non-toxic solvent. In addition, CO_2's use as a solvent is useful because of its environmentally friendly properties as a solvent. CO_2 has a low Global Warming Potential (GWP=1) and no Ozone Depleting Potential (ODP). Carbon Dioxide's unique characteristics differentiate it from other solvents, as it is: non-toxic, easily available, odorless, tasteless, inexpensive and non-flammable (Mukhopadhyay, 2000). Figure 5 shows the correlation between pressure and density at different pressures for CO_2. Supercritical CO_2 is unique in the fact that though it is a non-toxic gas at atmospheric conditions, it also has the ability to be a solvent with densities close to those of water under certain supercritical conditions. Comparing the density of supercritical CO_2 to the density of water at room temperature (around 1g/ml) seen at the top of Figure 5, under pressures close to 3,000 psi and at a temperature of 92 ºF supercritical CO_2 has the ability to act as a solvent with a density which is only 10% less than that of water.

Chapter 2: Background

The main focus of this thesis will be to experimentally determine CO_2's ability to act as a solvent in its supercritical state. Though supercritical CO_2's ability to be used as a solvent has already been researched and proven, the objective of the presented work is to further explore its properties as a solvent by building a prototype apparatus where CO_2 is utilized as a solvent to extract caffeine from coffee and collect data to explore CO_2's capability as a solvent for this application.

Table 2: Supercritical CO_2 Solubility (Mukhopadhayay, 2000)

Very Soluble	Sparingly Soluble	Almost Insoluble
Nonpolar and slightly polar low M.W. (<250) Organics, e.g., mono and sesquiterpenes, e.g., thiols, pyrazines, and thiazoles, acetic acid, benzaldehyde hexanol, glycerol, acetates	Higher M.W. organics,(<400), e.g., substituted terpenes and sesquiterpenes, water, oleic acid, glycerol, decanol, saturated lipids up to C_{12}	Organics with M.W. above 400, e.g., sugars, proteins, tannins, waxes, inorganic salts, chlorophyll, carotenoids, citric, malic acids, amino acids, nitrates, pesticides, insecticides, glycine, etc.

Table 2 provides more information regarding the solvent properties and selectivity of supercritical CO_2. Though certain solvents are specifically used for specific applications, Table 2 provides a clear understanding of the solvent capabilities of supercritical CO_2. Supercritical CO_2 would work well for the extraction of molecules with molecular weights less than 250 g/mol as stated in the "Very Soluble" column. This supercritical CO_2 apparatus was tested by extracting caffeine from coffee beans in order to determine the effectiveness of the designed apparatus. Since molecules with weights less than 250 g/mol are considered "very soluble" in supercritical CO_2, caffeine is well suited to be extracted with supercritical CO_2 because it has a molecular weight of 194.19 g/mol. Knowing that molecules with molecular weight greater than 400 g/mol are almost insoluble in Supercritical CO_2, as stated in Table 2, this makes supercritical CO_2 an

optimum solvent of choice for selective extractions. Supercritical CO_2 is often the solvent of choice in essential oil production and pharmaceutical research where a final product is required to be free from nitrates, insecticides, pesticides, waxes and or chlorophyll.

Table 3: Properties of CO_2 States (Taylor, 1996)

	Density (g/mL)	Dynamic Viscosity (g/cm-sec)	Diffusion Coefficient (cm^2/sec)
Gas (ambient)	0.0006–0.002	0.0001–0.003	0.1–0.4
Supercritical fluid (T_c, P_c)	0.2–0.5	0.0001–0.0003	0.0007
Liquid (ambient)	0.6–1.6	0.002–0.03	0.000002–0.00002

Additionally, CO_2 is an abundant industrial waste product, which is inert. Not only is supercritical CO_2 a safe, clean and plentiful solvent, but it also has many characteristics that are advantageous for extraction. For instance, CO_2's diffusivity is greater than other liquids by 10-100 times, allowing for faster mass transfer and shorter extraction durations than conventional liquid solvents (Mukhopadhyay, 2000).

Table 4: Supercritical CO_2 Properties (Taylor, 1996)

	CO_2^a	*n*-Hexane	Methylene Chloride	Methanol
Density (g/mL)	0.746	0.660	1.326	0.791
Kinematic viscosity ($m^2/s \times 10^7$)	1.00	4.45	3.09	6.91
Diffusivity of benzoic acid ($m^2/s \times 10^9$)	6.0	4.0	2.9	1.8

Table 4 shows the significant difference in kinematic viscosity, the ratio of dynamic viscosity to density, of supercritical CO_2 compared with n-Hexane and Methanol. Supercritical CO_2 has a 4 to 7 times lower kinematic viscosity when compared to these other two liquid solvents. These beneficial properties allow supercritical CO_2 as a solvent to not only have a high density but also a low viscosity allowing it to flow through mediums with less resistance and more diffusivity. CO_2's low surface tension enables it to more easily penetrate an extraction medium, making supercritical CO_2 an ideal solvent

for many applications throughout a wide range of industries. Figure 6 shows the schematic for a simple once through, open-loop supercritical CO_2 extraction test apparatus.

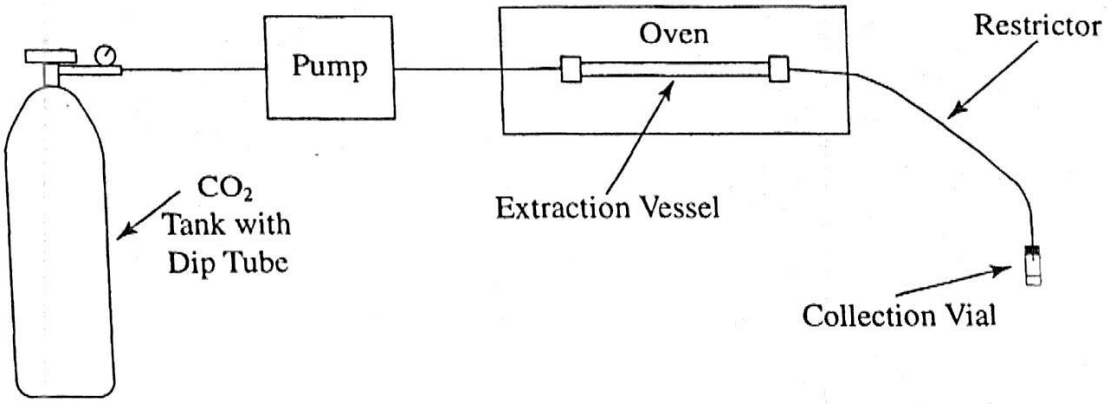

Figure 6: Simple Open-Loop CO_2 Extraction System (Thurman, 1998)

One of the most desirable properties of supercritical CO_2 is the fact that it leaves no residue due to the fact that it is a gas at ambient conditions; this unique characteristic allows supercritical CO_2 to be utilized in in both food and biomedical applications. Though supercritical CO_2 has a multitude of benefits over conventional organic solvents, the main barrier to the implementation of Carbon Dioxide's use as a solvent are the high initial costs to build a system which is able to successfully bring CO_2 up to its critical point for use as a solvent. However, the initial costs of building systems that implement supercritical CO_2 have not prohibited many companies from implementing supercritical CO_2 as a solvent for their industrial processing needs. Supercritical Carbon Dioxide is currently used in a multitude of industries including aerospace, microchip manufacturing, food production, biomedical, pharmaceutical, dry-cleaning, and many more (Mukhopadhyay, 2000).

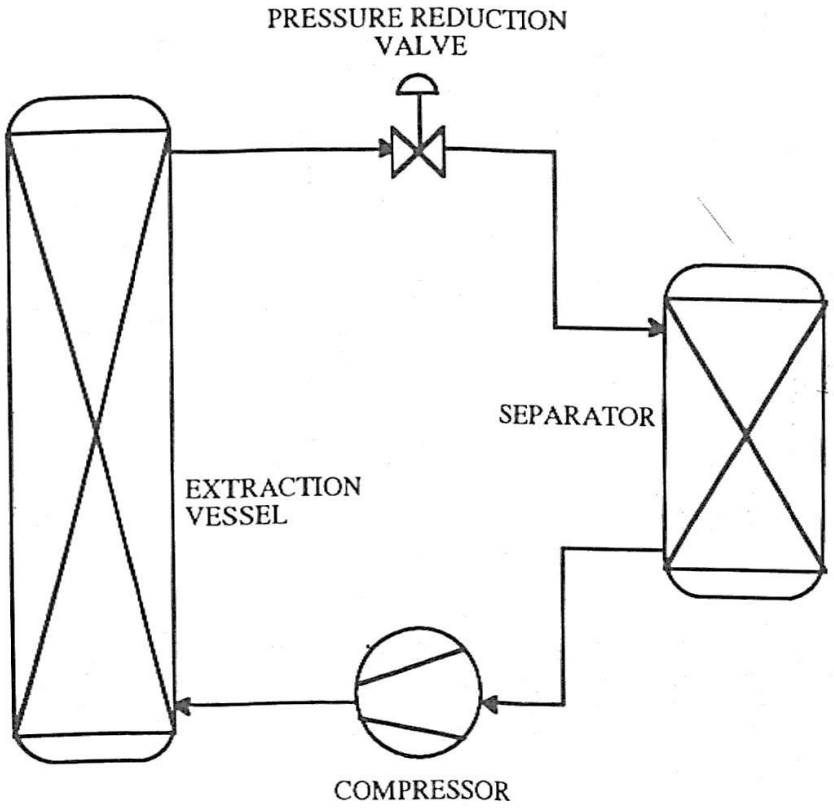

Figure 7: Simple Closed-Loop Supercritical CO_2 Extraction Cycle (McHugh, 1994)

This thesis investigates the feasibility of a low cost small-scale, closed-loop supercritical CO_2 extraction system by researching, designing, building and testing a supercritical CO_2 extraction apparatus. A simple schematic incorporating the system and four major components is shown in Figure 7. This project explores the solvent abilities of supercritical CO_2 by extracting caffeine from coffee. Also the apparatus examines potential ways to improve the efficiency of a system that utilizes CO_2 as a solvent. The following chapter presents a description and breakdown of the thesis apparatus, which describes the components as well as the overall system, design and function.

Chapter 3: Description

3.1 Main System Components:

3.2 Compressor

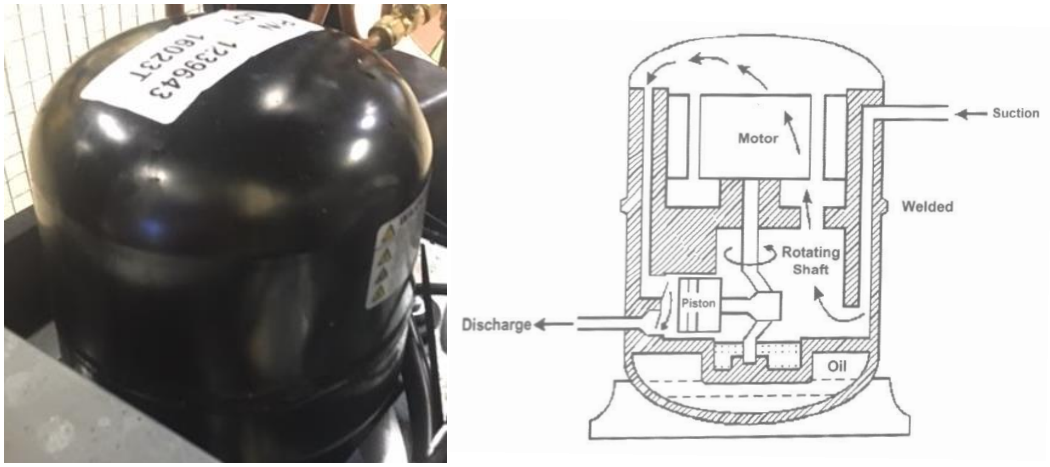

Figure 8: Hermetically Sealed Reciprocating Oil Lubricated Compressor

The compressor is what "drives" the supercritical extraction cycle and is the heart of the system. An internal schematic of this hermetically sealed compressor can be seen in Figure 8. The compressor is the most important part of the supercritical CO_2 system as it is what provides the necessary pressure lift in order for the CO_2 to reach the transcritical region. The equation for this pressure ratio is provided in Equation 1.

$$Pressure\ Ratio = \frac{Pdischarge}{Psuction} \quad (1)$$

The compressor component that is used in the apparatus is a Sanden transcritical CO_2 compressor model unit typically produced for refrigeration applications. The work done by the compressor, $\dot{W}_{in}$, is found using Equation 2, where $\dot{m}_{CO2}$ is the refrigerant mass flow rate and h_1 represents enthalpy of the saturated vapor entering the compressor and h_2 is the enthalpy at outlet of the compressor.

$$\dot{W}_{in} = \dot{m}_{CO2}(h_2 - h_1) \quad (2)$$

This compressor is one of the only small transcritical CO_2 compressors that is available in the United States for small-scale applications. The Sanden compressor used in the apparatus is oil-cooled and suitable for this thesis research, however would not be implemented in industrial applications. In industries that utilize supercritical CO_2 extraction (ie. Aerospace, biomedical, and pharmaceutical), an oil-free diaphragm compressor would be used as seen in Figure 9. A search for small oil-free transcritical CO_2 compressors revealed that the most cost-effective oil-free CO_2 compressor that would be available internationally would cost close to $29,000. Therefore, the Sanden compressor was used for this research.

Figure 9: Oil-free Diaphragm Compressor (Source: http://www.lewa-inc.com)

The compressor efficiency, η_c, is found by dividing the theoretical adiabatic compression by the actual compressor data. This is accomplished first calculating adiabatic compression assuming entropy at the inlet of the compressor is equal to the entropy at the outlet of the compressor with no heat transfer, resulting in enthalpy values for h_1 and h_{2s}. The theoretical enthalpy value given no heat transfer is then divided by the actual enthalpy value, h_2, which is measured by the pressure and temperature data at the

compressor outlet. Using these measurements Equation 3 can be implemented to find the compressor efficiency.

$$\eta_c = \frac{h_{2s} - h_1}{h_2 - h_1} \quad (3)$$

The compressor inlet receives low pressure CO_2 vapor from the low- pressure separation tank. In order to ensure that no particles of coffee bean or skin are carried past the low-pressure separation tank, the low-pressure side of the compressor must stay below the supercritical pressure of 1080 psi. The high-side pressure on the outlet of the hermetically sealed Sanden positive displacement reciprocating compressor needs to maintain a pressure of 1080 psi or higher in order to maintain the CO_2 in its transcritical region to act as a solvent. There is an increase in temperature in both the compressor and in the actual CO_2 at the outlet of compressor due to the work being done on the CO_2 gas in the compressor. This heat will be removed from the compressor by a fan, and the heated CO_2 will be cooled by the next component: the gas cooler.

3.3 Gas Cooler

Figure 10: Gas Cooler

The gas cooler as seen in Figure 10, can also be thought of as similar to a condenser due to the fact that they both act as heat exchangers transferring heat out of the system. The difference in name is due to the fact that in a transcritical system the gas cooler only reduces the temperature of the CO_2 and cannot condense the CO_2 no matter how much heat it removes. The gas cooler is a heat exchanger that rejects heat from both the work of the compressor and the heat added through the low pressure separation vessel. The gas cooler that is being used is produced by Sanden, the same company that produced the compressor. This gas cooler, normally used for refrigeration systems, rejects heat to the ambient air with the help of forced convection induced by a fan. Due to the fact that the system is not trying to cool a contained space like a refrigeration cycle, the system was designed to use this excess heat in order to help provide heating to the low temperature side around the separation vessel. In order to accomplish this alternative function of the gas cooler, the gas cooler was placed into a container filled with water so that it would transfer heat from the high pressure and high temperature gas into the surrounding water. The heat transfer rate of the gas cooler, $\dot{Q}_{Gas\ Cooler}$, is found using Equation 4, where $\dot{m}_{CO2}$ is the refrigerant mass flow rate and h_2 represents enthalpy of the vapor leaving the compressor and h_3 is the enthalpy at outlet of the gas cooler.

$$\dot{Q}_{Gas\ Cooler} = \dot{m}_{CO2}(h_2 - h_3) \qquad (4)$$

The gas cooler was designed with enough surface area in order to transfer heat from the work of the compressor to the surrounding air, therefore the gas cooler has more than enough surface area to transfer the necessary heat into the water in the heat exchanger bath. The gas cooler is an important part of the thesis apparatus as it is the component that controls the density of the supercritical CO_2 entering into the extraction chamber. With the ability to cool the temperature of the CO_2 in the gas cooler by circulating low temperature water from the low-pressure separation vessel, the system is

in theory able to lower the temperature of the gas cooler and therefore the density of the supercritical CO_2 passing through it. Since CO_2 has a wide range of densities in the transcritical region, by cooling the supercritical fluid in the gas cooler it is possible to have a fluid with density similar to water flowing through the extraction chamber.

3.4 High Pressure Supercritical Chamber (HPSC)

The high-pressure supercritical chamber (HPSC) that was suitable for this particular system design was manufactured by Temprite, a company that specializes in transcritical CO_2 refrigeration equipment. For the system specifications, the HPSC needed to be able to handle pressures up to 1,500 psi working pressure, while also having the ability to be repeatedly easily opened in order to access the inside of the chamber. The necessary equations for calculating pressure vessel wall thickness can be seen in Tables 5 & 6.

Table 5: Pressure Vessel Wall Thickness Equations (Lindeburg, 2013)

member	minimum thickness,[a] t	maximum pressure, p	limitation
(in terms of inside radius) longitudinal joint (circumferential stress)	$\frac{pR}{SE - 0.6p}$	$\frac{SEt}{R + 0.6t}$	$p \leq 0.385SE^{b}$ $t \leq 0.5R$
(in terms of inside radius) circumferential joint (longitudinal stress)	$\frac{pR}{2SE + 0.4p}$	$\frac{2SEt}{R - 0.4t}$	$p \leq 1.25SE$ $t \leq 0.5R$
(in terms of outside radius, R_o) longitudinal joint (circumferential stress)	$\frac{pR_o}{SE + 0.4p}$	$\frac{SEt}{R_o - 0.4t}$	$p \leq 0.385SE$ $t \leq 0.5R$

Table 6: Pressure Vessel End Cap Wall Thickness Equations (Lindeburg, 2013)

head type	minimum thickness, t	maximum internal pressure, p	limitation
thin hemispherical			
(inside radius)	$\frac{pR}{2SE-0.2p}$	$\frac{2SEt}{R+0.2t}$	$p \leq 0.665SE$
(outside radius)	$\frac{pR_o}{2SE+0.8p}$	$\frac{2SEt}{R_o-0.8t}$	$t \leq 0.356R$
ellipsoidal*			
(inside diameter)	$\frac{pDK}{2SE-0.2p}$	$\frac{2SEt}{KD+0.2t}$	$K=\frac{1}{6}\left(2+\left(\frac{D}{2h}\right)^2\right)$
(outside diameter)	$\frac{pD_oK}{2SE+2p(K-0.1)}$	$\frac{2SEt}{KD_o-2t(K-0.1)}$	$K = 1$ for 2:1 ellipsoidal heads

The HPSC chamber seen in Figure 11 holds the material which the system will be removing components from via the supercritical flow through the vessel. Thus, the chamber needed to contain a screen mechanism in order to prevent larger material from being carried out of the vessel and into other components of the system, which could block flow or cause damage to the entire system.

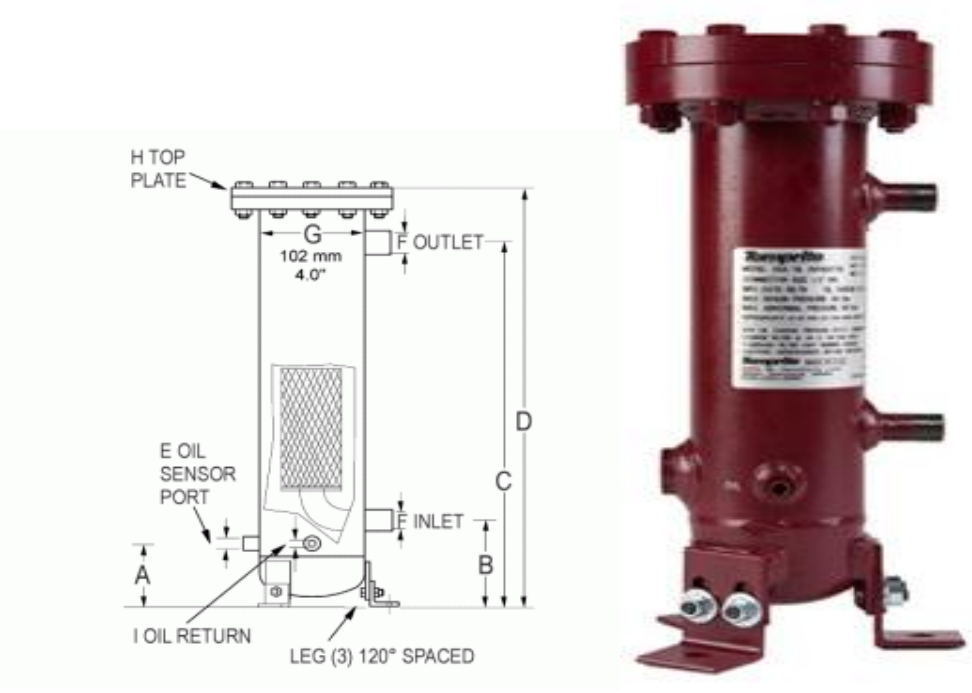

Figure 11: High Pressure Supercritical Chamber (Source: http://temprite.com)

3.5 Expansion Valve

The expansion valve seen in Figure 12 is the component that causes the pressure difference between the high and low side of the system. The velocity of the flow through the valve can be determined using Equation 5, where, ΔP, is the pressure differential and C is a constant which is experimentally measured and provided by the manufacture for each specific valve.

$$V = C\sqrt{2(\Delta P)} \quad (5)$$

Due to the fact that this apparatus works under large pressure differentials with high pressure (approximately 1,500 psi) on one side and low pressure (approximately 300 psi) on the other side, the expansion valve needed to be rated to work under these extreme conditions. Not only did the expansion valve need to meet these operating parameters, but since most expansion valves use a small needle to create an orifice through which the fluids flows and as a result a pressure drop occurs, a unique design had to be implemented with this extraction apparatus. The mass flow through the valve can be determined using Equation 6, where, A, is the cross-sectional area of the valves orifice and ρ is the density of supercritical fluid.

$$\dot{m} = \rho A V \quad (6)$$

There will be intentional impurities in the gas including particulates flowing through the valve. A regular needle valve would increase the risk of clogging, so it is necessary that a high differential pressure rated diaphragm valve be used. The diaphragm valve will allow orifice adjustability in order to set the pressure differential, while reducing risk of clogging or seizing due to particulate buildup on the threads.

Figure 12: Swagelok Diaphragm Expansion Valve

3.6 Low Pressure Separation Tank (LPST)

The low-pressure separation tank (LPST) shown in Figure 13 is exactly the same component as the high-pressure tank and is therefore rated for operation at high pressures; thus, the low pressure separation tank has a higher factor of safety because it is rated for higher pressures then it will be subjected to in the system operation. The main considerations for the HPSC were also true for the LPST, regarding both accessibility and filtration. The main difference between the HPSC and LPST is the exterior water jacket used to warm the vessel. Since the LPST will be at a low temperature (between 15-50 °F), it will use a water loop connected to the gas cooler as a heat exchanger in order to

help warm the cool LPST. The heat transfer rate of the water jacket on the LPST, $\dot{Q}_{H2O}$, is found using Equation 7, where $\dot{m}_{H2O}$ is the water mass flow rate, c_p, is the specific heat of water and T_1 represents the temperature of the water at the inlet of the warming jacket while T_2 is the temperature of the cooled water at the jacket outlet.

$$\dot{Q}_{H2O} = \dot{m}_{H2O} \bullet c_p(T_2 - T_1) \quad (7)$$

If the water jacket circulating warm water from the gas cooler does not provide enough BTUs of heat, then an additional heater will be placed on the tank in order to help heat the flashed liquid CO_2 into gas. If there is not enough heat to achieve a phase change from liquid CO_2 into gaseous CO_2, the system will eventually lose pressure and liquid CO_2 could enter the compressor causing damage. The LPST seen in Figure 13 allows the CO_2 to drop in pressure and return to a gas and liquid phase mixture instead of supercritical CO_2. Since the CO_2 will no longer be a solvent at this pressure, it will no longer be able to carry any of the particulates that it extracted from the first vessel, and the pressure drop will cause the non-solvent CO_2 to drop the extracted substance to the bottom of the low pressure separation tank.

Figure 13: Low Pressure Separation Tank with Exterior Water Jacket Heat Exchanger

3.7 Coalescers

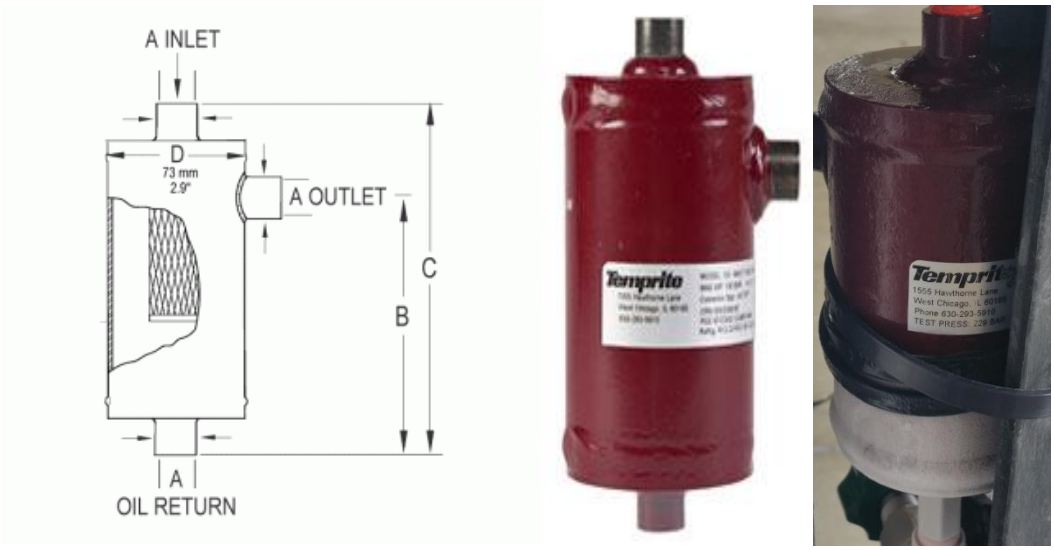

Figure 14: Coalescer Particulate Filters (Source: http://temprite.com)

The system has two oil coalescers as seen in Figure 14 in order to prevent damage to the system. The first oil coalescer is located after the compressor in order to recapture the oil particulates that have escaped from the compressor and return these particulates back to lubricate the compressor. This oil coalescer will serve two functions; firstly, it will primarily ensure that the compressor maintains lubrication, especially since the apparatus requires opening, closing and depressurization of the system. In order to determine the terminal velocity, V_t a few calculations must first be completed. The superficial fluid velocity, V, is found using Equation 8, where, D is the internal diameter of the separation vessel and, Q is the volumetric flow rate inside of the vessel.

$$V = \frac{Q}{\pi D^2/4} \qquad (8)$$

Using the superficial fluid velocity, V, from Equation 8, the Reynolds number, Re, will be found using Equation 9. In Equation 9, D is the internal diameter of the separation vessel, ρ_f is the density of the fluid and μ is the fluid viscosity.

$$Re = \frac{VD\rho}{\mu} \quad (9)$$

The Reynolds number calculated from Equation 9 can then be used to reference an associated drag coefficient, C_D, from Table 7.

Table 7: Variation of Drag Coefficient with Reynolds Number for a Sphere

Reynolds Number	Drag Coefficient
1	30.0
10	4.0
100	1.1
1000	0.4

The terminal velocity can calculated using Equation 10, where, g is gravitational acceleration, d, is the critical droplet diameter, C_D, is the dimensionless drag coefficient and, ρ_v is the density of the vapor. Equation 9 shows the simplified formula for determining the terminal velocity of the CO_2 droplets in the separation vessel.

$$V_t = \sqrt{\frac{4gd(\rho_f - \rho_v)}{3\rho_v C_D}} \quad (10)$$

The second function of this oil coalescer is to prevent as much oil as possible from entering into the rest of the system. In order to ensure that analytical tests are accurate regarding the amount of extracted material in the separation tank, it was necessary to prevent any oil from accumulating in the separation tank. The second oil coalescer is located after the separation tank in order to ensure that no unwanted particulates from the HPSC or LPST end up in the compressor. Any kind of impurities that are caught in the flow and carried into the compressor can cause damage to the piston and result in seizing or decreased pressure differential performance.

Chapter 4: Testing

4.1 Design Considerations

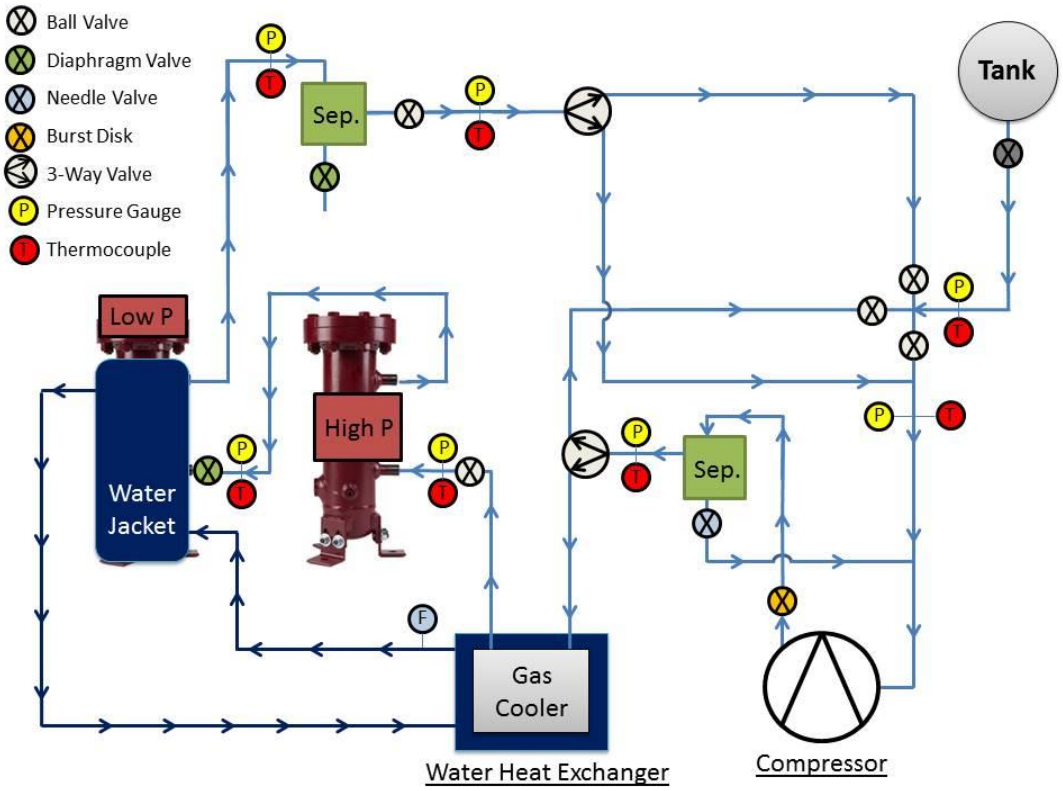

Figure 15: Schematic of Prototype CO_2 Extraction System

The goal of this thesis was to build an apparatus in order to be able to analytically explore, test and determine the efficiency of using supercritical CO_2 as a solvent. There are very few companies in the United States that utilize transcritical CO_2. This project was not only limited by the small availability of companies to work with, but also that many of the companies in this field only work on a large scale industrial level. The goal of the thesis design was to be safe, maneuverable, interchangeable, accessible and as easy to operate as possible. In order to achieve this, an industrial cart was implemented as the

frame for the 275 pound system. Due to the weight and size of the system each and every component not only had to be secure but also accessible.

The small compact design was achieved by using every bit of usable space and implementing flexible high-pressure hoses with stainless steel quick disconnect fittings for quick assembly in compact spaces. The system not only had to be self-contained within the cart but also had to be easily operated and monitored. This was achieved by designing the system so that all of the valves and monitoring equipment would be isolated and easily accessible on the top tier of the cart. Not only did the design have to be safe, secure, and maneuverable but it also had to accurately monitor and record all necessary data throughout operation. This was achieved through a design which incorporated gauges, thermocouples, energy meters as well as a flow meter and scale all built in throughout the system in order to gather all of the necessary data for both safety and data collection.

4.2 Bill of Materials

This extraction system includes various groups of components that can be separated by their function within the system. The hoses, valves and fittings required for the supercritical CO_2's flow path of operation signifies the first group. The second grouping of parts includes the digital gauges, thermocouples, and the associated data acquisition equipment necessary for measurements. Finally, the last group is all of the remaining parts necessary for the system to function.

A bill of materials with detailed costs can be found in the Appendix A. The Bill also includes relevant information for each individual product.

4.3 Hoses and Fittings

For many refrigeration systems copper piping is used, however for this supercritical system high pressure hoses were implemented. The hoses utilized in this apparatus are all rated for working pressures of 3000 psi and allow for flexibility in the apparatus.

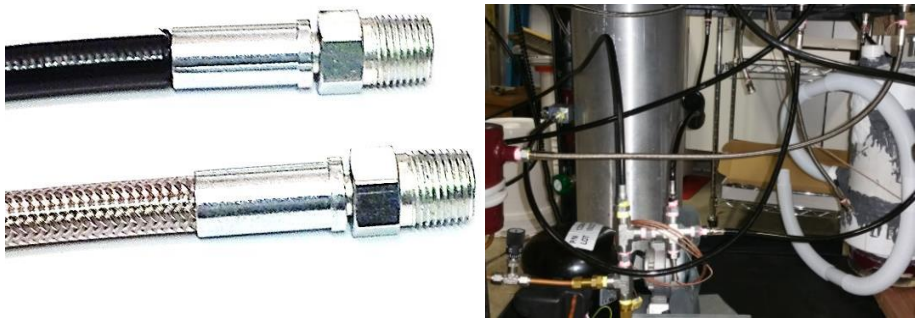

Figure 16: High Pressure Supercritical CO_2 Hoses

The decision to use high pressure hoses instead of piping was in order to allow for easy adaptability and changes to be made on this system, so that each component could potentially be replaced, exchanged or moved if necessary. Since this supercritical system is charged and discharged each time that the system is run, it was necessary to provide access in order to allow moving, changing or replacing of each system component. The hoses are important for both maintenance and for providing the ability to open both the high and low side pressure vessels for making adjustments to ensure that the apparatus is running properly.

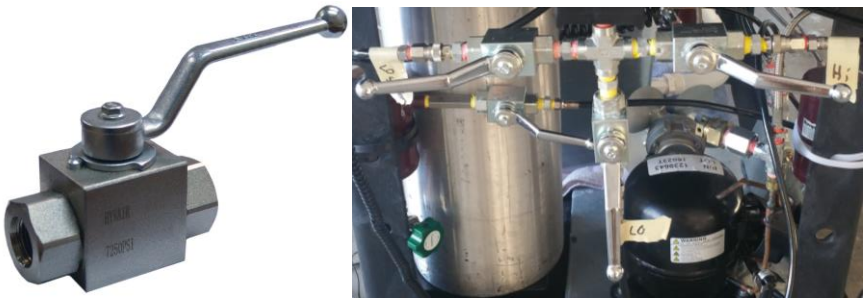

Figure 17: High Pressure Ball Valves

In order to safely and easily control the flow of the CO_2 in the system, high pressure 2- and 3-way valves, rated for operation of 5,000 psi, were implemented. In order to make sure that the valves were easy to manipulate as well as easy to identify with respect to valve position, high pressure valves with long handles as seen in Figure 16 shows the 2-way valve implemented in the system. These high pressure ball valves allowed for quick visual inspection as well simple opening and closing while the system was operating.

With every connection wherever possible in the system stainless steel unions, tees, and reducers were used in order to ensure that each fitting was rated for working pressures significantly higher than the system would ever endure. Having a factor of safety with each of the individual parts used to build the apparatus was part of the safety plan in order to prevent any failure and ensure safety throughout operation. A list of fittings used in this system can be found in Appendix A in the Bill of Materials with information on the type of fitting and its rated working pressure.

4.4 Gauges, Thermocouples, Displays and Accessories

In order to ensure safety and collect all necessary data, this system implemented 7 locations where both the CO_2's pressure and temperature were recorded. All digital gauges were implemented in the design of the apparatus in order to allow quick readability of pressures from any angle or distance.

Figure 18: Digital Pressure Gauge

The digital gauges utilized in this apparatus are rated for operation up to 2,000 psi and have an accuracy of +/- 5 psi. Though this design only requires 2 gauges to safely monitor the high and low pressure sides, the design implemented 7 gauges throughout the system in order provide the ability to monitor pressure at each component and ensure that there were no pressure pockets in the system for safety. Since this system is made up of separate components and systems under high pressure a blockage or closed valve in any component could cause pressure to rise in a specific area quickly causing a potential safety hazard. This potential hazard was mitigated and addressed through the use of multiple pressure gauges measuring pressures in each component ensuring safety.

Figure 19: High Pressure Thermocouple Probe

Since this system operates under high pressure it was determined that thermocouples rated for 2,500 psi with NPT connections would be used in the system in order to guarantee stable, reliable and leak free thermocouple connections. Two data loggers with large LCD screens were selected in order to easily monitor and record the temperatures. These temperature loggers allowed for quick and easy real time readability during operation for safety.

Figure 20: 4-Channel DAQ

4.5 Water Heat Exchanger

Figure 21: Water Loop Heat Exchanger

Along with CO_2 data collection, due to the fact that the heat exchanger water loop is essential in determining system performance throughout operation, a third Arduino data logger with a smaller real time temperature display was implemented to record and plot data from the water loop. These thermocouples took recordings of the water inlet, outlet as well as at different areas of the gas cooler throughout each of the data collection runs. These additional thermocouples provided the ability to monitor temperature creep in the system over time. Lastly, in order to determine overall heat exchanger effectiveness and heat transfer, the water flow rate was measured using a turbine flow meter. Due to the fact that CO_2 reaches such a low temperature at the expansion device, a backup heating element was implemented surrounding the low pressure expansion tank. This heating element ensured that there was enough heat load in order to evaporate any accumulated liquid CO_2 in the Low Pressure Separation Tank. Since the system components were initially designed to work in a refrigeration application, where the compressor cycles on and off to maintain a certain set-point temperature, it was necessary to ensure that there was enough heat load on low temperature side of the system to maintain system performance.

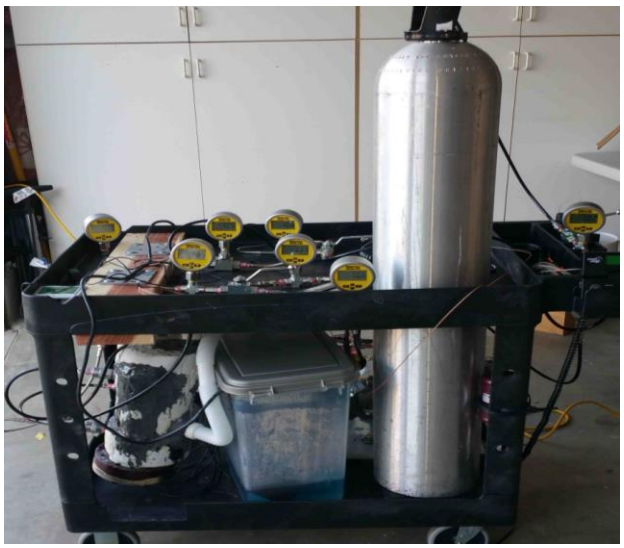

Figure 22: Thesis Apparatus

4.6 Supercritical CO_2 Extraction Cycle

The main components of the prototype are similar to those of a basic refrigeration system. A basic refrigeration system is comprised of: a compressor, condenser, expansion valve and evaporator. The main differences between the prototype and a refrigeration system are that: (1) the condenser is called a gas cooler, (2) the evaporator takes the form of the low pressure separation vessel, and (3) an additional high pressure supercritical chamber is placed in the system. Similar to the process of any refrigeration cycle, the apparatus' process relies on the compressor to drive fluid flow through the system while the expansion valve serves the purpose of creating the pressure differential. The gas cooler and flash tank provide heat transfer between the high side and low side of the system. The theoretical steady state flow of this system can be seen in Figure 23.

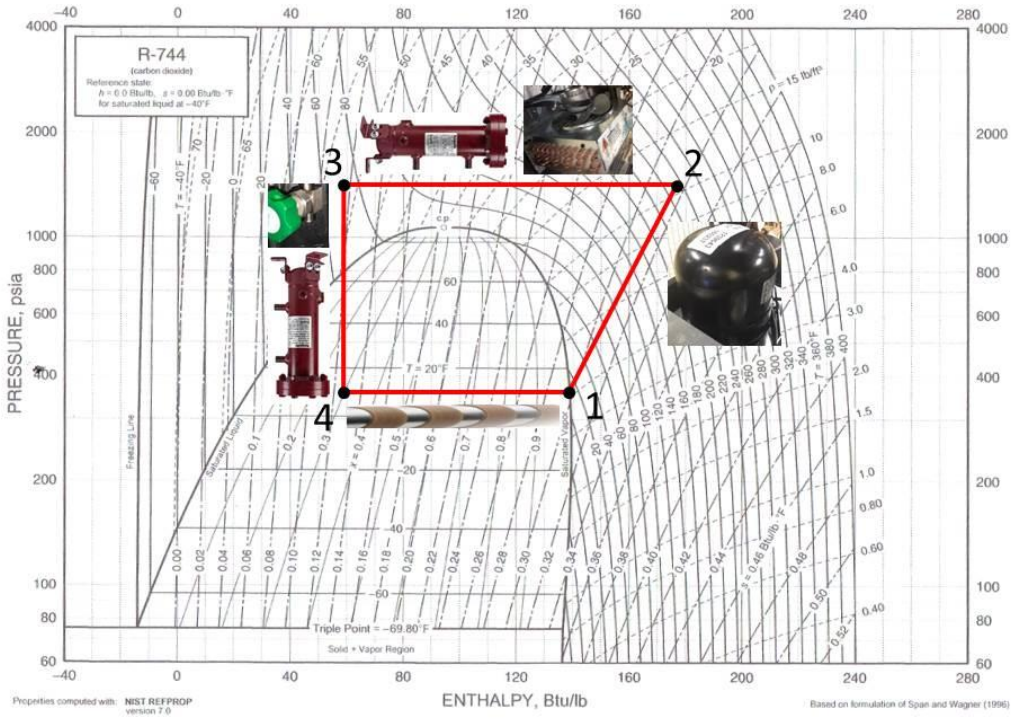

Figure 23: Pressure-Enthalpy Diagram of Supercritical Process

Figure 23 shows the Pressure-Enthalpy diagram of this system under steady state operation and ideal operating conditions. In the figure, different system components can be seen alongside their associated portion of the supercritical extraction process. Starting at the bottom right of the cycle, the compressor increases the CO_2 pressure and temperature. The high pressure, high temperature gas is then cooled through the gas cooler before flowing through the material in the high pressure supercritical chamber. At point three the supercritical fluid then drops in pressure as it passes through the expansion valve. The CO_2 liquid and gas mixture of a certain quality then enters the low pressure separation tank where heat is added to the system through a heating element. The CO_2 gas then flows back to the compressor at state 1 where the process begins again.

4.7 Equipment Safety and Operation

Although carbon dioxide is nontoxic, it is odorless and colorless, so it is virtually impossible to tell if there is CO_2 being released by the system. In order to account for this, the system was operated in a well ventilated environment and a CO_2 monitor was implemented in order to track CO_2 concentration and provide alarms to ensure the carbon dioxide levels do not exceed 1000 ppm in the surrounding environment per ASHRAE standards. This monitor is located at the base of the unit near the floor to provide the most accurate, worst case scenario since carbon dioxide is heavier than air and it will accumulate near the ground. In addition to all of these safety precautions, the apparatus was also thoroughly tested under pressure for leaks using a mixture of soap and water in order to identify and secure any locations leaking CO_2.

4.8 CO_2 Recovery & Discharging the Unit

Due to the nature of this apparatus which requires charging the system with a large amount of CO_2, certain precautions have been taken. First, a system operation was

developed in order to recover as much CO_2 as possible once the experimental data was collected. This CO_2 recovery is achieved by redirecting the flow from the compressor into the CO_2 tank. The goal of the project was to have the ability to recapture 50-75% of the CO_2 used in the experiment. The two points which need to be closely monitored in the recapturing process are the tank pressure and inlet temperature into the tank. After the apparatus recovers as much CO_2 as possible, and the tank pressure is higher than the system pressure, the remaining CO_2 in the system must be discharged. When discharging, the room must be well ventilated as mentioned in the paragraph above. Also, since CO_2 levels will be monitored and logged for safety, the discharge process should be done slowly in order to prevent high CO_2 concentrations in the surrounding environment as well as to prohibit flashing and loss of compressor oil due to rapid depressurization. The next section outlines the step-by-step process for operating the apparatus.

4.9 Operation

1. Before pressurizing the system, check to ensure the diaphragm valve for depressurizing system is closed. Using line of sight, visually walk down the flow of CO_2 through the system and make sure that all valves are open to allow flow.

2. Once the open status of the flow path is confirmed, the system can be pressurized from the CO_2 tank. Slowly open the main valve on the CO_2 tank and allow the pressure of the system to equilibrate with the pressure in the tank. This should be done slowly in order to minimize shock on the pressurizing system. (Due to safety and system performance, the CO_2 tank is on a scale to monitor the amount CO_2 added into the charged system.)

3. Once the system and tank reach equal pressures (between 700-900 psi depending on ambient temperature), close the valve to the tank and allow the system to sit and

equilibrate in temperature with the surrounding environment. (This is an important step in the process to ensure safety. In order to ensure there is no liquid in the compressor, the CO_2 tank needs sufficient time to warm back up to ambient temperature. If this step is overlooked, this could result in damage when the compressor is turned on.)

4. Once everything has reached equilibrium in pressure and temperature, the system is ready to start. Begin the system by turning on power to the compressor, which will be seen by an instantaneous increase in pressure on the high side. Then, slowly open the main valve from the CO_2 tank in order to charge the system. (As the CO_2 tank is opened, there will be in increase in pressure on both the high and low pressure sides however the differential should remain around the same.)

5. If necessary adjust the expansion valve on the low pressure expansion tank in order to keep the low pressure side of the system slightly lower than the tank pressure in order to maintain flow from the tank for charging the system.

6. Closely monitor the pressure around the system while charging. Make sure to slowly cycle the main CO_2 tank value slightly open and closed to allow the system to charge followed by equilibration until the system is fully charged (around 7 lbs CO_2).

7. Once the system is fully charged and the high side pressure is consistently above 1080 psi, the system can be run as long as desired in order to test specific operating times or conditions.

8. Make sure to continuously monitor pressure throughout the system, ensuring that the high pressure remains below 1,800 psi and the low pressure remains between 950 and 200 psi. Also, it is important to continue to monitor temperature at the compressor outlet to make sure that it is not above safe operating temperatures. The temperature

must also be monitored after the low pressure expansion vessel in order to ensure that liquid CO_2 is not a substantial portion of the low pressure expansion tank. (It is important that the compressor only receives gas at the inlet or this could result in damage to the compressor.)

9. Once the unit is done being run and the data is collected, the CO_2 recovery process will begin.

10. The CO_2 recovery is a three-step process, which begins by closing the expansion valve between the high and low pressure side. This will cause the high side to begin to increase in pressure, which is why the compressor must be turned off as soon as the valve is closed.

11. Next, redirect the 3 way-valve located on the high pressure side of the system from the gas cooler towards the main manifold and tank. Also, the two low pressure valves on the main manifold must be closed before the high pressure side valve to the CO_2 tank main valve can be opened, followed by opening the CO_2 tank main valve. This will cause the high pressure CO_2 to flow into the tank and equilibrate in pressure. Due to the flow into the tank, the CO_2 tank will increase in temperature. It is necessary to wait for the pressures to equalize and for the CO_2 tank to return to atmospheric temperature before proceeding with the next step.

12. Once pressure has equalized, the compressor will be used to pump the CO_2 back into the reservoir tank. This is accomplished by first opening the expansion valve of the separation tank as much as possible. Then, turning on the compressor and monitoring the pressure of the tank as well as throughout the system.

13. Once the high and low pressure sides have a large enough pressure differential that the compressor is no longer charging the tank, close the CO_2 tank main valve

followed by turning off the compressor. Once this is complete wait for the system to equilibrate in pressure.

14. Once the system has reached a resting pressure, the system charge can slowly be released. Before doing this close the valve between the oil coalescer on the low side and the compressor. (This provides more distance between the expansion valve opening and the compressor which is filled with oil). Once this valve has been closed, slightly open the diaphragm valve on the small oil coalescer after the low pressure separation tank until you begin to hear the CO_2 slowly escaping. This process should be done slowly as to not allow any of the oil from the compressor to flash and escape during the depressurization process.

15. Due to losses in system pressure throughout the process, the valve opening will have to be gradually opened more throughout the depressurization in order to continue to let the CO_2 gas escape. Once the valve is fully opened and all of the pressure gauges read zero, the system is still not ready to be opened and needs to rest for 1 hour. This resting time at ambient conditions allows for any liquid CO_2 which could have formed during depressurization to turn back into gas and safely escape the system.

16. Once the system has been resting for the necessary amount of time. The extraction and separation vessels can be safely opened and inspected.

A total of three operational runs were completed in thesis. Table 8 shows the summery for the operational parameters for each of these three runs. Run 1, was completed as a dry run without any coffee beans inside of the extraction vessel. During run 2 the extraction vessel was filled with green coffee beans and the system ran at the highest pressures of all three runs. Lastly, for run 3 roasted coffee beans were placed inside of the extraction vessel and a lower extraction pressure was tested.

Table 8: System Operation Summary

		Charge		Difference		Pressures (Psi)	
		In	**Out**			**Minimum**	**Maximum**
Run 1	**Fill**	5.31	4.06	1.25	lbs.	337	1276
Run 2	**Beans**	1412	1412	0	grams	605	1495
	Fill	6.44	5.19	1.25	lbs		
Run 3	**Beans**	723	732	(+9)	grams	423	1164
	Fill	5.1	3.4	1.75	lbs		

Chapter 5: Results

5.1 Run 1

The first run of the system after completing all of the pressure testing was done with an empty system, without coffee beans, in order to ensure safe operation. Table 1 shows the initial CO_2 charge in the system as well as the recovered CO_2 after run 1.

Table 9: Run 1 System Charge & Recovery

	In	Out	Difference	
Fill	5.3125	4.0625	1.25	lbs

Table 10: Run 1 System Operation Pressures

Start	High	Low
2:20	1276	377
3:20	1211	365
4:40	1173	354
5:20	1105	337

Table 2 shows the operating pressures of the system over the period of the 3 hour test run. This first run was successful in achieving pressures above 1080 psi in the high pressure extraction vessel creating supercritical CO_2. The pressure difference seen in Table 6 is almost exactly what would be seen by this compressor when used in its intended refrigeration application. Over the 3 hour period of operation, there is a continuous change in pressure in the overall system pressure. The high pressure side drops 171 psi while the low pressure side drops 40 psi over operation. After confirming there was no leak in the system during operation, the source of this pressure loss was identified with the low pressure separation tank. This will be further discussed throughout this section. Figure 24 shows the system flow schematic along with the locations of data acquisition in the system flow.

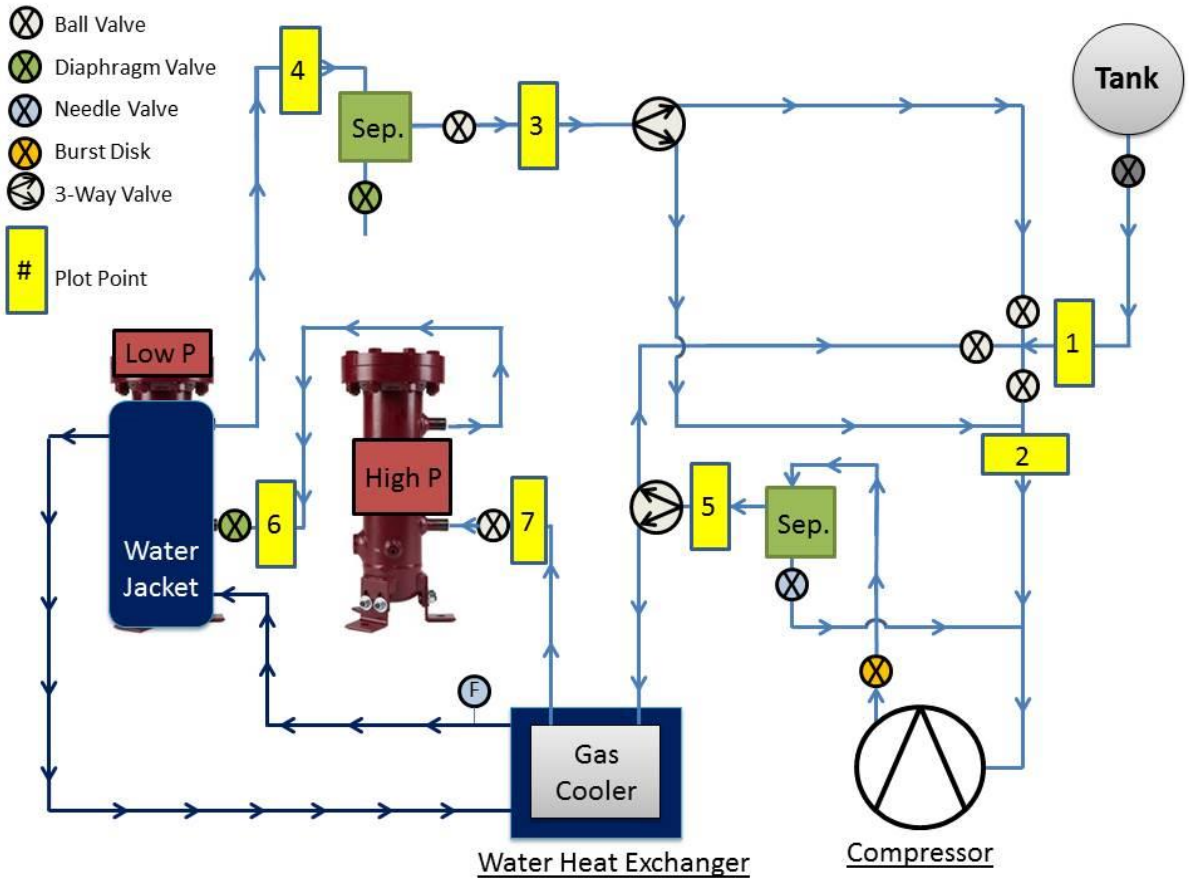

Figure 24: Flow Schematic with temperature Data logging Locations

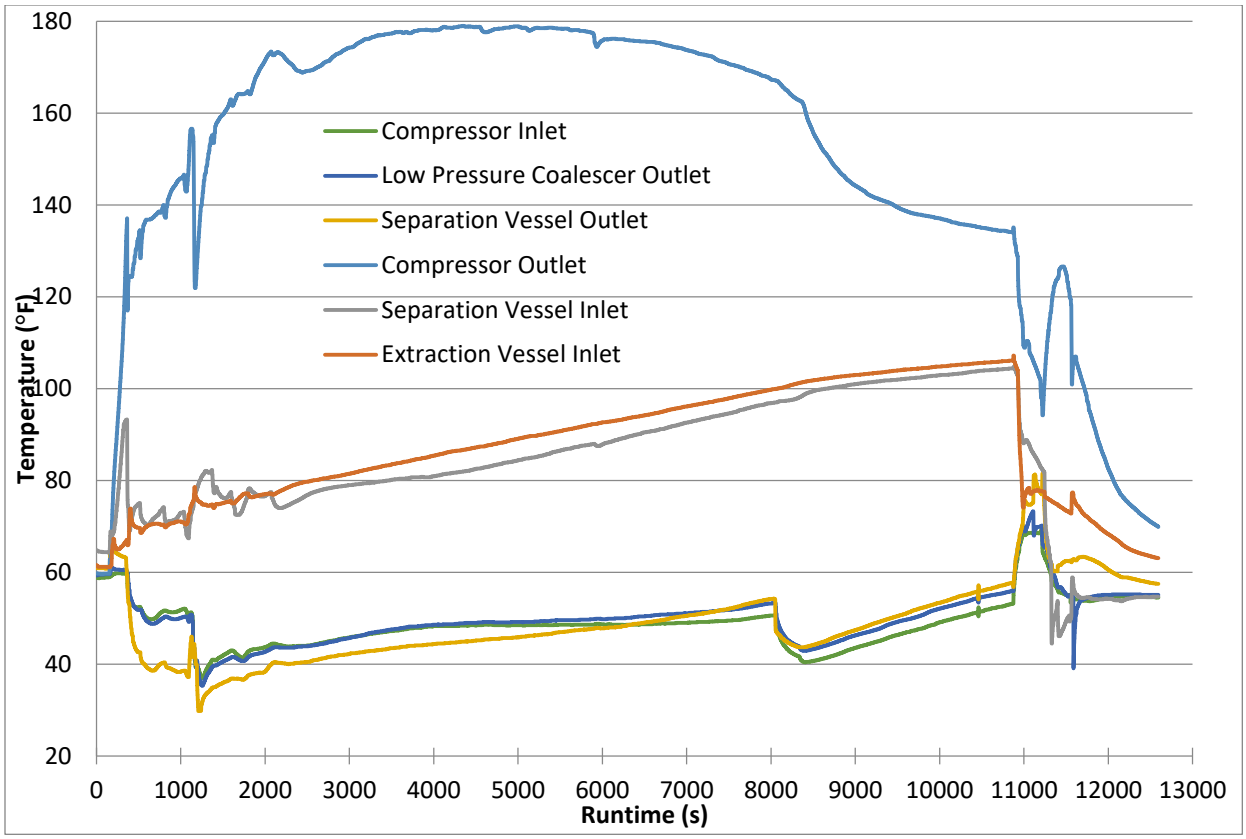

Figure 25: Run 1 Temperature Plot

Figure 25 is a plot of the recorded system operating temperatures over run 1 of the system and shows the temperature differential resulting from the operating pressure differential. The initial starting point can be seen on the left side of the plot with initial starting temperatures of around 60 °F. The temperature of the compressor outlet quickly rises to above 130 °F within the first two minutes of operation as seen by the blue line. Though the temperature of the compressor rises quickly initially, it eventually settles operating between 170 °F and 180 °F for a majority of operation. One interesting aspect shown on this plot are two periods during startup where there are significant temperature drops in of compressor outlet temperature, from 137 °F to 117 °F and 156 °F to 122 °F. These discrepancies in the smooth plot of the compressor outlet temperature profile were most likely a result of liquid CO_2 entering into the compressor inlet. This correlation can be clearly seen in Figure 25 after a run time of 1000 seconds, with the drop in

temperatures of series 2 and 3 followed by the significant drop in the series 5 compressor outlet temperature.

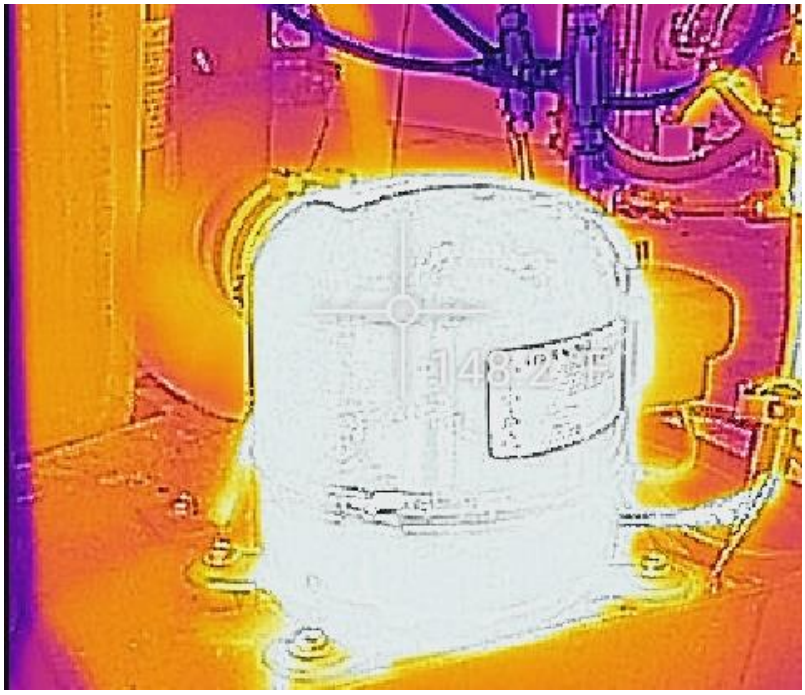

Figure 26: Thermal Image of Compressor

The low pressure side of the system can be seen by the plots of the compressor inlet, low pressure coalescer outlet and the separation vessel outlet temperatures in Figure 25. The low pressure side temperatures do not vary as drastically as the compressor outlet. This is what would be expected since the temperatures are closer to the initial starting temperature. While observing the temperatures over time of the low pressure side there is a slight temperature creep. The low pressure side temperatures initially start around 40 °F and slowly make their way up to around 50 °F throughout the operation of the unit. This is an average increase of 0.083 °F per minute while operating. There is a 13 °F drop in the low pressure temperatures from 53°F to 40°F around runtime 8,000 which was a result of closing the expansion valve in order to maintain supercritical pressure in the high pressure vessel. This tightening of the expansion valve seemed to affect both temperature on the low pressure side and the temperature of the compressor outlet

however it did not seem to make a difference in the temperature of the CO_2 after the gas cooler or in the supercritical vessel. This is also what would be expected since the water loop heat exchanger is driving the temperature of the gas cooler, and it is not able to respond instantaneously to temperature change due to its thermal mass.

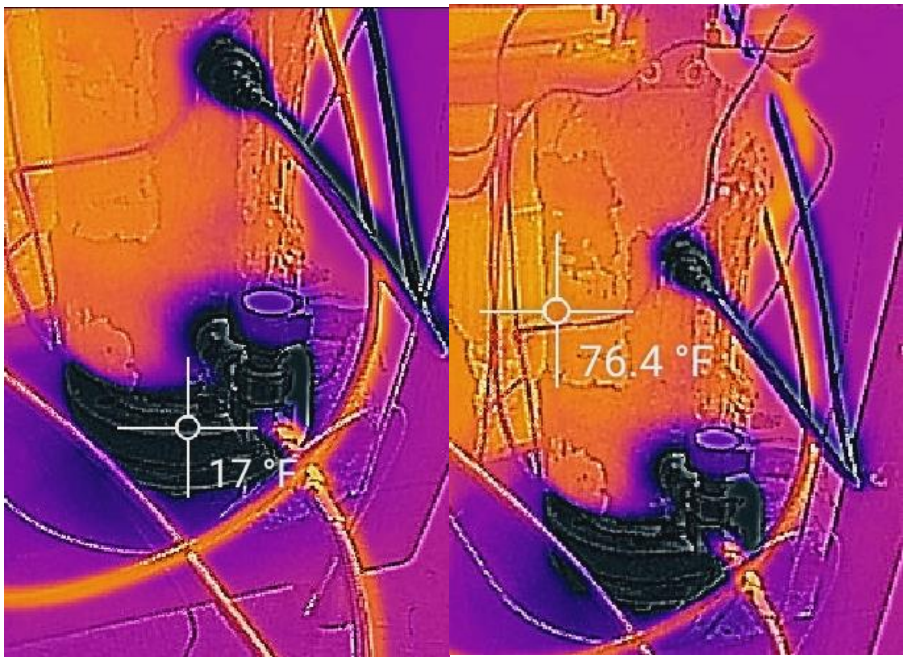

Figure 27: Thermal Image of Low Pressure Flash Tank and Expansion Valve

The expansion valve was tightened, as seen by the dip on the low pressure side temperature, in order to keep pressure in the supercritical chamber above 1080 psi. Since this was the first operation of the apparatus, it was found that the heat exchanger was not as effective as planned in the design. As a result of this the separation vessel after the expansion valve was not being provided with enough heat load. This resulted in the accumulation of liquid CO_2 in the vessel over time, taking away from the overall CO_2 charge in the rest of the system and therefore resulting in overall system pressure loss.

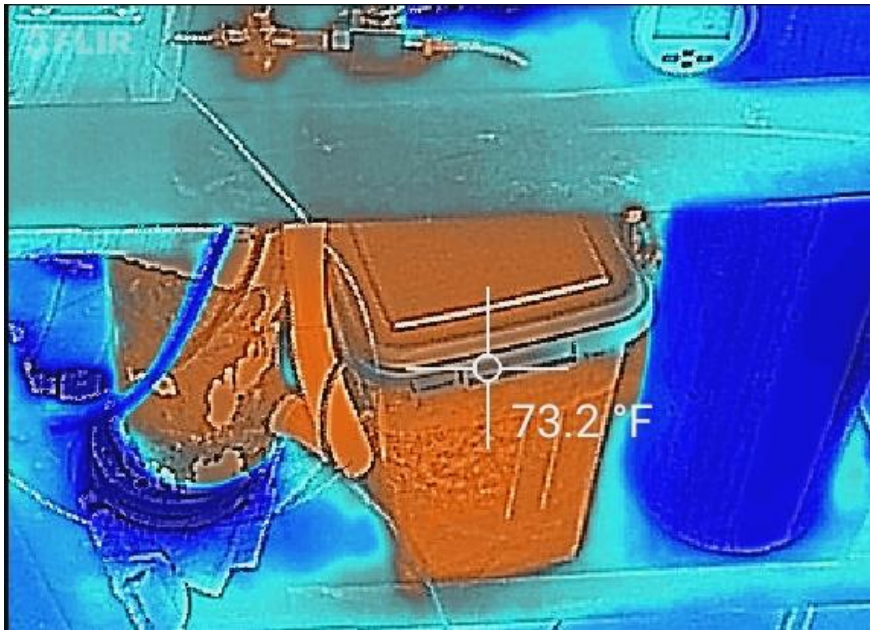

Figure 28: Thermal Image of Water Heat Exchanger, High and Low side

Figure 28 shows the temperature difference between the gas cooler on the high side and the low pressure expansion tank on the left side of the photo. Unfortunately, there was a malfunction in the water heat exchanger data acquisition during the first run and as a result it was only possible to save data from the last two minutes of operation. Figure 29 shows the plotted water heat exchanger data with a 1.8 °F temperature difference between the inlet and outlet temperature. With this limited information it was not possible to track the overall temperature creep in the water heat exchanger throughout run 1 however using the flowrate measured of 4 GPM, the average heat exchange rate of 3,600 BTU/hr was determined.

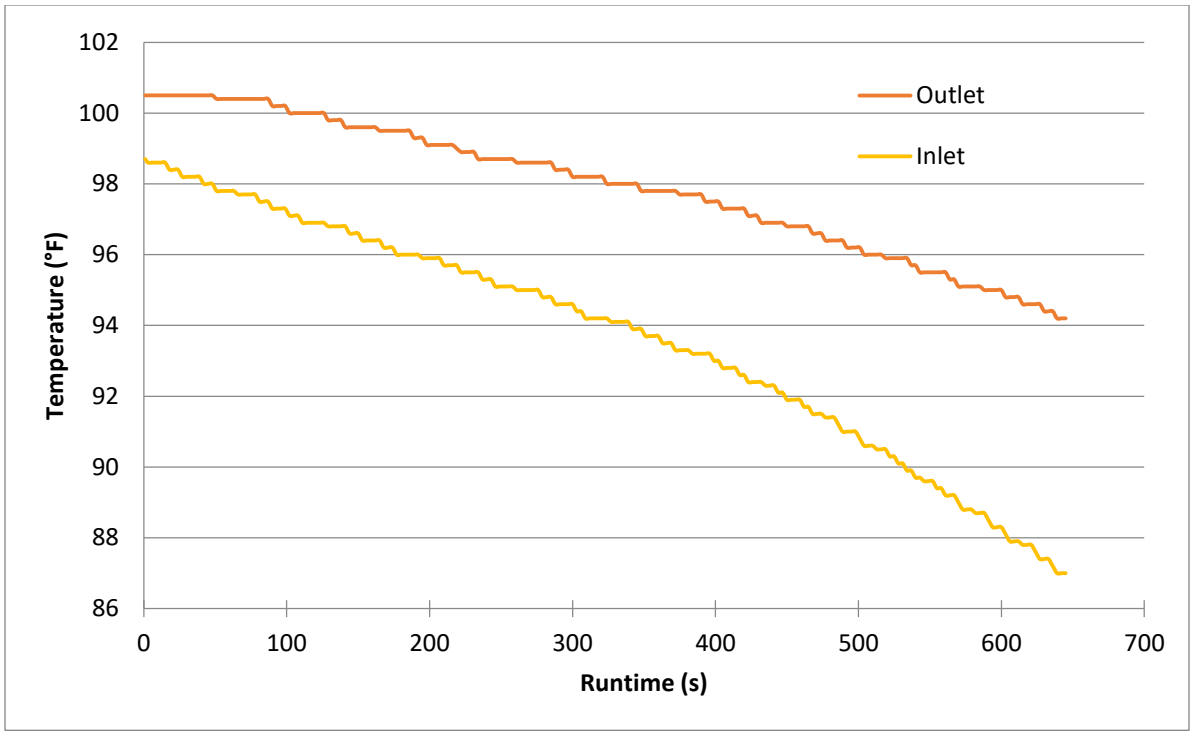

Figure 29: Run 1 Heat Exchanger Temperatures

The plotted temperatures of the separation vessel inlet and the extraction vessel inlet in Figure 25 show the significant temperature creep of the system over the period of operation increasing an average of 0.31 °F per minute. The temperatures at the extraction vessel inlet and outlet are the most important temperatures to focus on controlling for supercritical CO_2 extraction due to the fact that they dictate the density of the supercritical fluid which is flowing through the extraction chamber. This is one of the variables which will determine overall extraction effectiveness and efficiency. Based on the conditions from the start of operation until the end of operation, the density of the supercritical CO_2 after the gas cooler and in the extraction vessel begins at 52.8 lb/ft^3 and slowly decreases in density until the end of the run at 44.4 lb/ft^3.

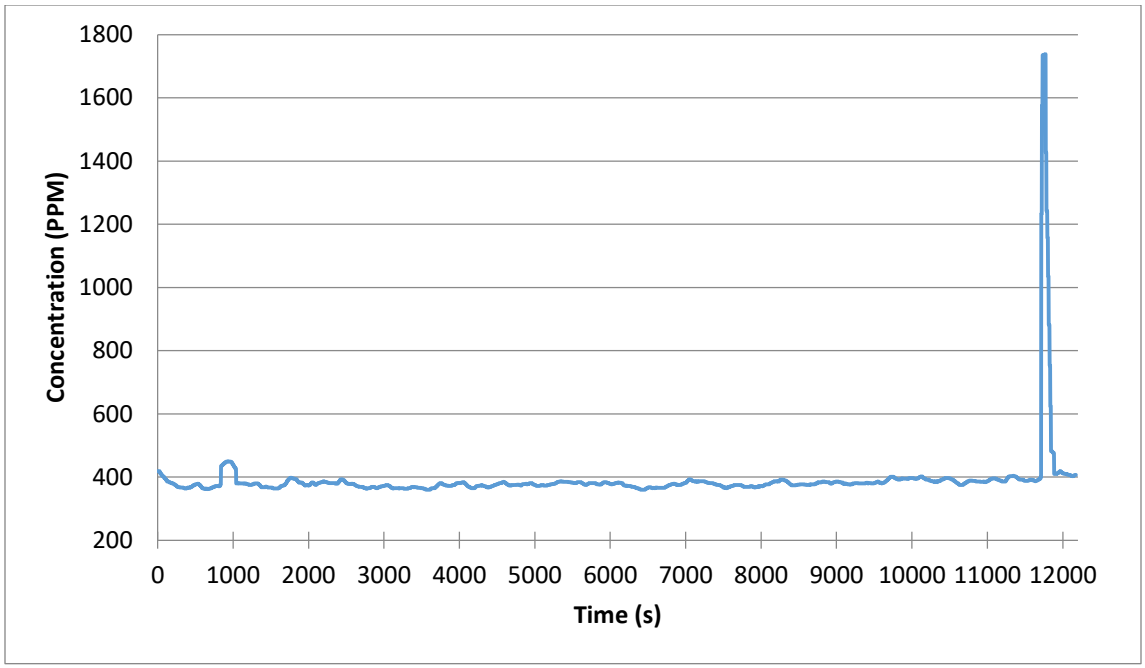

Figure 30: Run 1 CO_2 Concentrations

Figure 30, shows CO_2 levels in PPM throughout the duration of the first run. In order to monitor the work environment and ensure that safe CO_2 levels were maintained a CO_2 environmental monitor meter was placed inside of the cart. Figure 30 shows that throughout operation the CO_2 in the operating environment was within normal safe levels between 375-400 ppm. The significant spike in CO_2 concentration at the end of the plot was a result of depressurization. This data was skewed as it was the first time using the monitor and the monitor was located within one foot of the system discharge location. Though there is a spike in CO_2 concentrations, the levels peak for 2 minutes, which was the time it took to realize the mistake in location and move it to the other side of the cart in order to provide a more accurate reading of the CO_2 concentration in the environment.

5.2 Run 2

The second run of the system was done with the extraction vessel full of green coffee beans. Table 7 shows the weight of green coffee beans in the system before and after extraction along with the system CO_2 charge and recovery amounts.

Table 11: Run 2 System Charge & Recovery

	In	Out	Difference	
Beans	1412	1412	0	grams
Fill	6.4375	5.1875	1.25	lbs

As seen in table 7, there was no caffeine extracted from the green coffee beans. Though the extraction was not successful on the first attempt valuable information was gathered by tracking the performance of the system during this second run. Table 8 includes operating times and system pressures throughout the run which were higher then run 1 due to the increase in system CO_2 charge. Over the 2 hour period of operation, there is a continuous pressure rise in the overall system pressure. The high pressure side increases a maximum of 175 psi while the low pressure side increases 295 psi over the entire run 2 operation.

Table 12: Run 2 System Operation Pressures

Start	High	Low
2:20	1320	605
2:50	1340	630
3:20	1400	662
3:50	1495	755
4:20	1400	900

Though this second run did not result in the extraction of caffeine, the system did maintain supercritical CO_2 in the extraction vessel despite significant fluctuations in

compressor operation throughout the run time. Figure 31 is a plot of the recorded system operating temperatures over run 2 of the system.

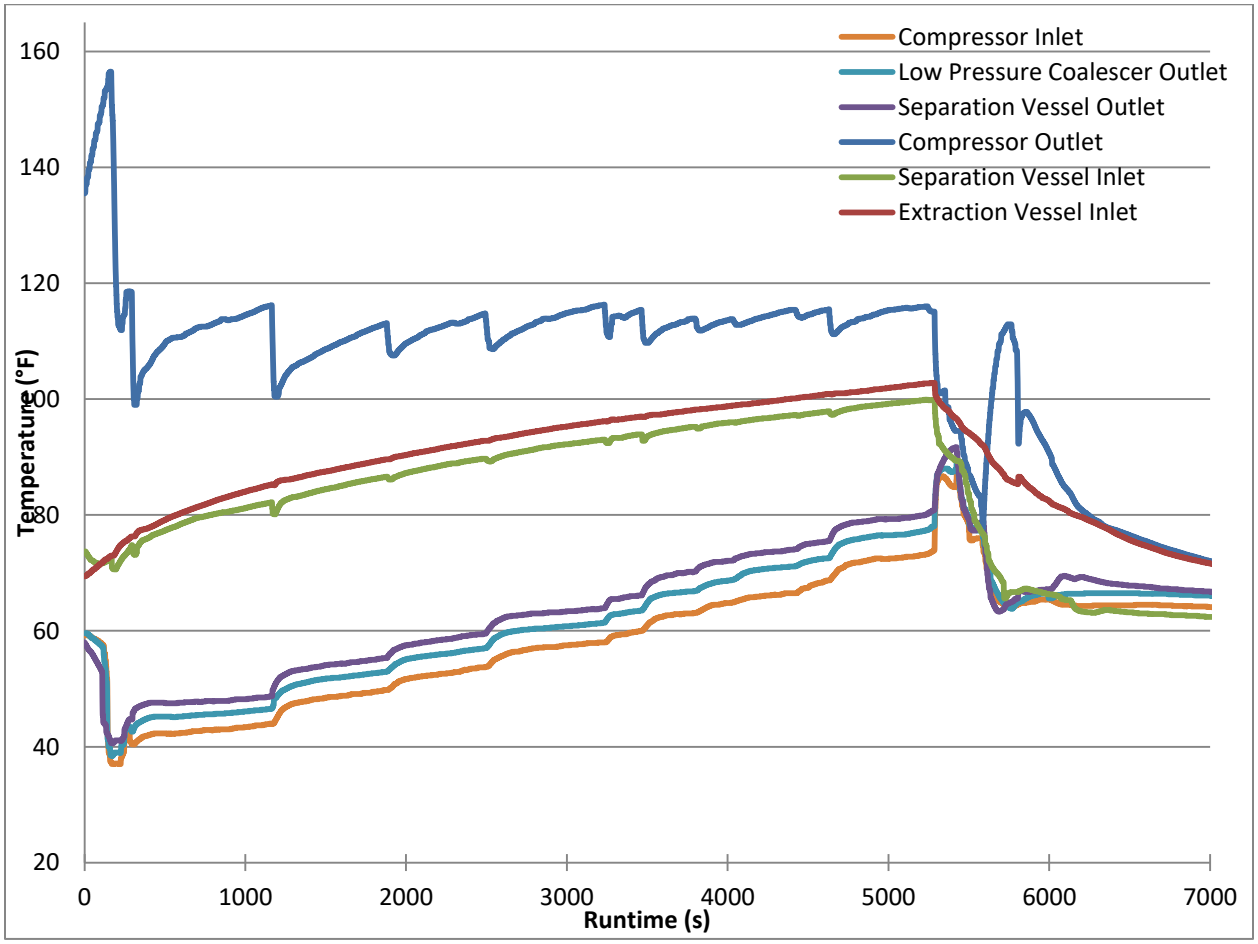

Figure 31: Run 2 Temperature Plot

The starting point of the system for run 2 can be seen on the left side of the plot with initial starting temperature of the system around 70 °F. The temperature of the compressor outlet quickly rises to above 150 °F, seen by the plot of the compressor outlet temperature which quickly drops off falling to 110 °F. Though the temperature of the compressor rises quickly initially, it eventually settles operating between 100 °F and 115 °F for a majority of operation. Due to the compressor rating, it would be expected that the compressor would run at its initial temperature around 150 °F over the entire operation and therefore the plot of the blue line around 110 °F, shows that compressor is not

operating normally during this run. Interpreting the data, there is a possibility that liquid was entering the compressor, leading to internal cooling and a lower exit temperature at the compressor outlet. This possibility was determined by plotting the inlet temperature and pressure of the compressor on a Pressure Enthalpy diagram which clearly showed the state at the inlet of the compressor in the saturated region of the P-H dome. While operating the unit, the compressor outlet temperature seemed low however there were no audible or physical differences in system operation from the first run other than compressor outlet temperature. This operation of the compressor with liquid in the inlet is likely the cause of damage which resulted in the compressors short operational life.

The low pressure side of the system can be seen in Figure 31 in the plots of compressor inlet, low pressure coalescer outlet and the separation vessel outlet temperatures. The low pressure temperatures for run 2 show significant temperature creep over run 2 operation moving from 38 °F to 73 °F resulting in an increase of 0.4 °F / min. This temperature creep is a direct result of the implementation of a heater on the low pressure separation vessel during run 2. The heater was implemented on run 2 after there was not enough heat load on the low temperature separation vessel during run 1 which resulted in difficulty maintaining system pressure. In order to solve this problem a silicone tape heater was implemented around both the bottom of the low pressure separation vessel and the expansion valve. A thermal image of this heating element around the low pressure separation vessel can be seen at the bottom left side of Figure 32.

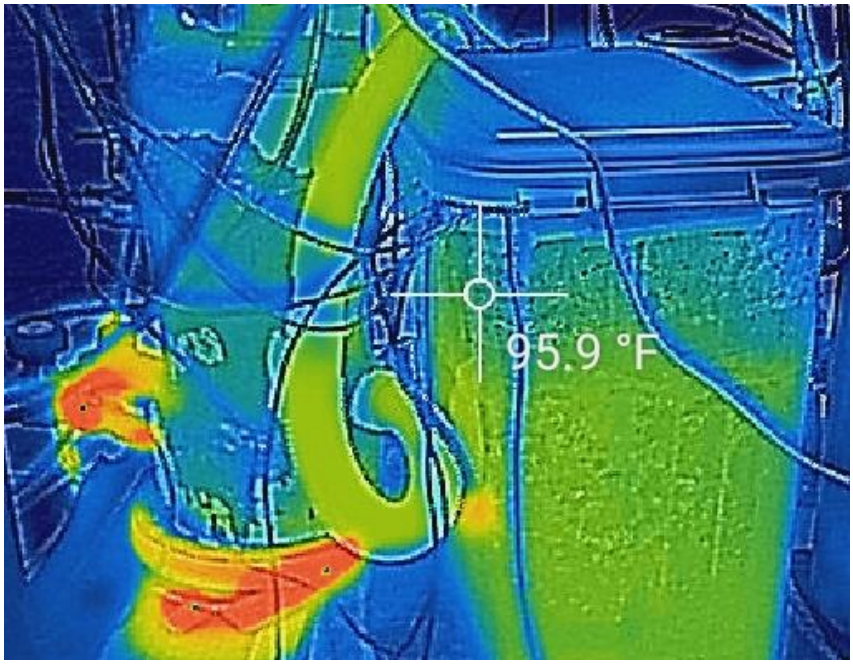

Figure 32: Thermal Image of Low Pressure Separation Vessel with Heater tape

This heater element placed on the separation vessel not only resulted in significant temperature creep on the low pressure side but also in the water heat exchanger loop seen in the Figure 33.

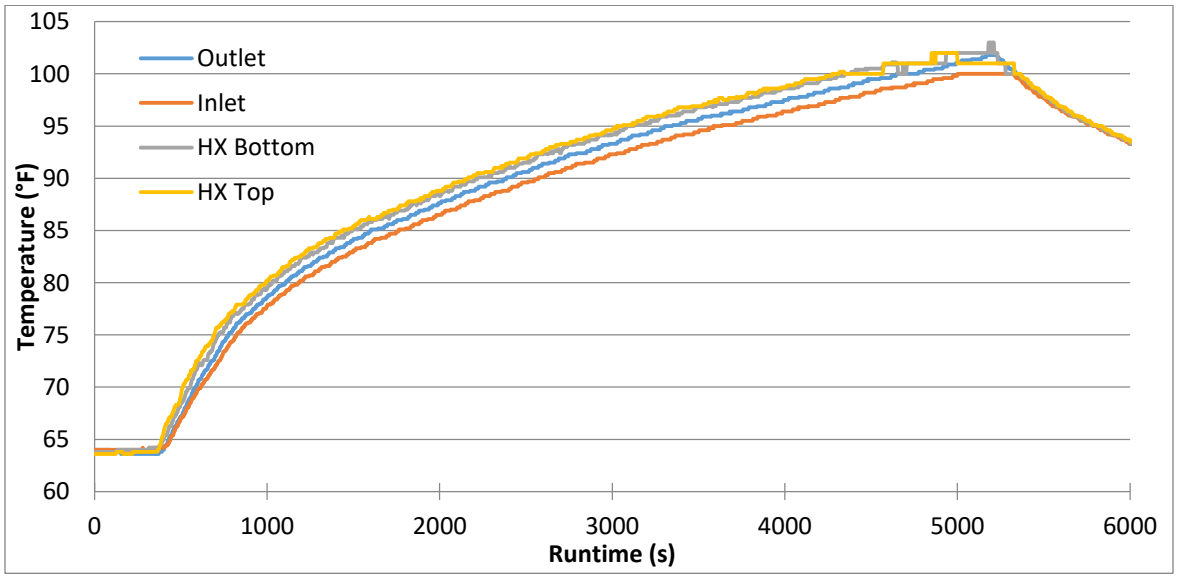

Figure 33: Run 2 Heat Exchanger Temperatures

Figure 33 shows the plot of the heat exchanger temperature throughout run 2 operation, showing a clear rise in system temperature throughout operation. The initial water starting at 64 °F quickly rises to 85 °F before continuing to increase up past 100 °F before the end of the second run. The data provides a 2.8 °F temperature difference between the inlet and outlet temperature and using the measured flowrate of 4 GPM, he average heat exchange rate of 4,600 BTU/hr was determined.

The plotted temperatures of the separation vessel inlet and the extraction vessel inlet in Figure 21 show the significant temperature creep in the supercritical fluid after the gas cooler over the period of operation increasing an average of 0.38 °F per minute. This rate in rise of temperatures is quicker then run 1 as a result of the additional heating element on the low pressure separation tank. The resulting increase in temperatures of series 6 & 7 causes a significant change in the density of supercritical CO_2 which is following through the extraction vessel. Based on the pressure and temperature of the operating conditions from the start of until the end of operation, the density of the supercritical CO_2 after the gas cooler in the extraction vessel begins at 50.9 lb/ft^3 and decreases in density until becoming less half the original density at 21.7 lb/ft^3 by the end of the second run. Due to the high operating temperature of supercritical fluid after the gas cooler in the extraction chamber Figure 34 shows a clear temperature distribution in the supercritical chamber using a thermal imaging camera.

Figure 34: Thermal Image of Supercritical Chamber Run 2

Figure 35 shows CO_2 levels in PPM throughout the duration of the second run. In order to continue monitoring the environment, ensuring that safe CO_2 levels were maintained the environmental CO_2 monitor was placed next to the apparatus on the opposite side of the depressurization valve. The plot in Figure 35 shows that throughout operation the CO_2 in the operating environment was within normal safe levels at around 400 ppm. The spike in CO_2 concentration at the end of the plot is a result of depressurization. The depressurization spike seen in run 2 is significantly lower than the one seen in run 1 due to the new location of the CO_2 monitor. With total instantaneous maximum CO_2 concentration of 577 ppm, this plot shows the apparatus well within safe environmental operating parameters throughout the entire operation.

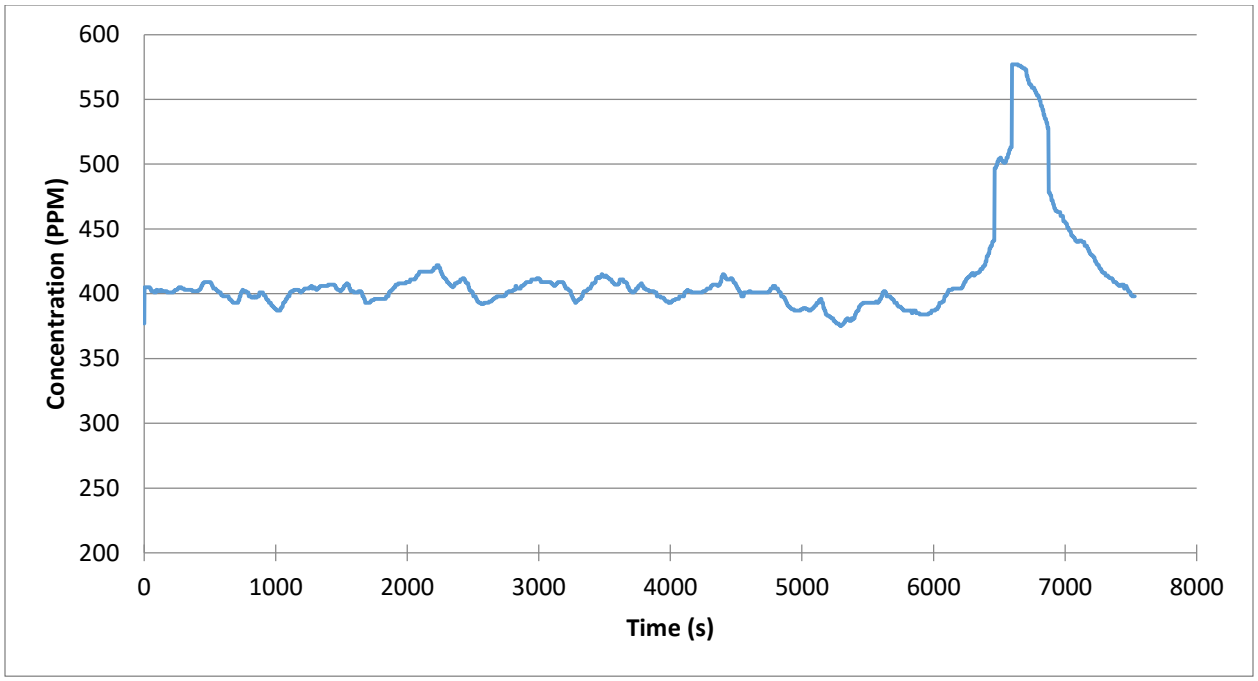

Figure 35: Run 2 CO_2 Concentrations

5.3 Run 3

The third run of the system was done with an extraction vessel full of roasted coffee beans. The table below shows the weight of the roasted coffee beans in the system before and after extraction along with the system CO_2 charge and recovery amount.

Table 13: Run 3 System Charge & Recovery

	In	Out	Difference	
Beans	723	732	(+9)	grams
Fill	5.125	3.375	1.75	lbs

As see from the table 9, the coffee beans weighed more after the extraction process then they did before they went in. After completing the system CO_2 recovery and depressurization, the removed coffee beans rested for an hour before being removed from the extraction vessel. Although the beans showed no initial signs of any difference, it became evident that there was still CO_2 trapped inside of the roasted beans. After weighing them, as the beans rested in the room they began cracking and popping as if they were popcorn being roasted over a fire. The release of CO_2 from inside of the beans caused them to crack loudly and continued for more than 12 hours throughout the night and into the next morning.

Table 14: Run 3 System Operation Pressures

Start	High	Low
6:20	1164	438
6:50	1141	447
7:20	1123	456
7:50	1157	428
8:20	1139	423

Table 10 includes operating times and system pressures throughout the run. Over the 2 hour period of operation, the overall system pressure remains relatively constant.

The high pressure side only fluctuates by a maximum of 41 psi while the low pressure side increases by only 18 psi over the entire run 3 operation.

On this third run the apparatus successfully extracted caffeine from the roasted coffee beans. Upon cleaning out the separation vessel, a total of 1 gram of material was collected from the separation vessel. The Ethiopian coffee beans which were implemented as the matrix to be extracted from in this thesis contain around 1% caffeine on average (https://www.coffeechemistry.com). Since the supercritical chamber was filled with 723 grams of coffee at 100% extraction efficiency, an extraction of 7.23 grams of caffeine would be expected. Since this system removed 1 gram of caffeine and coffee oils, this system during run 3 was most likely between 5% and 10% efficient. Unfortunately, there are no readily available consumer products for analytically testing the caffeine concentration of a substance other than expensive Gas Chromatography analysis. Therefore the exact caffeine concentration and composition collected from this run is unattainable however the extracted product can be seen in the Figure 36.

Figure 36: Coffee Oil and Caffeine Extract

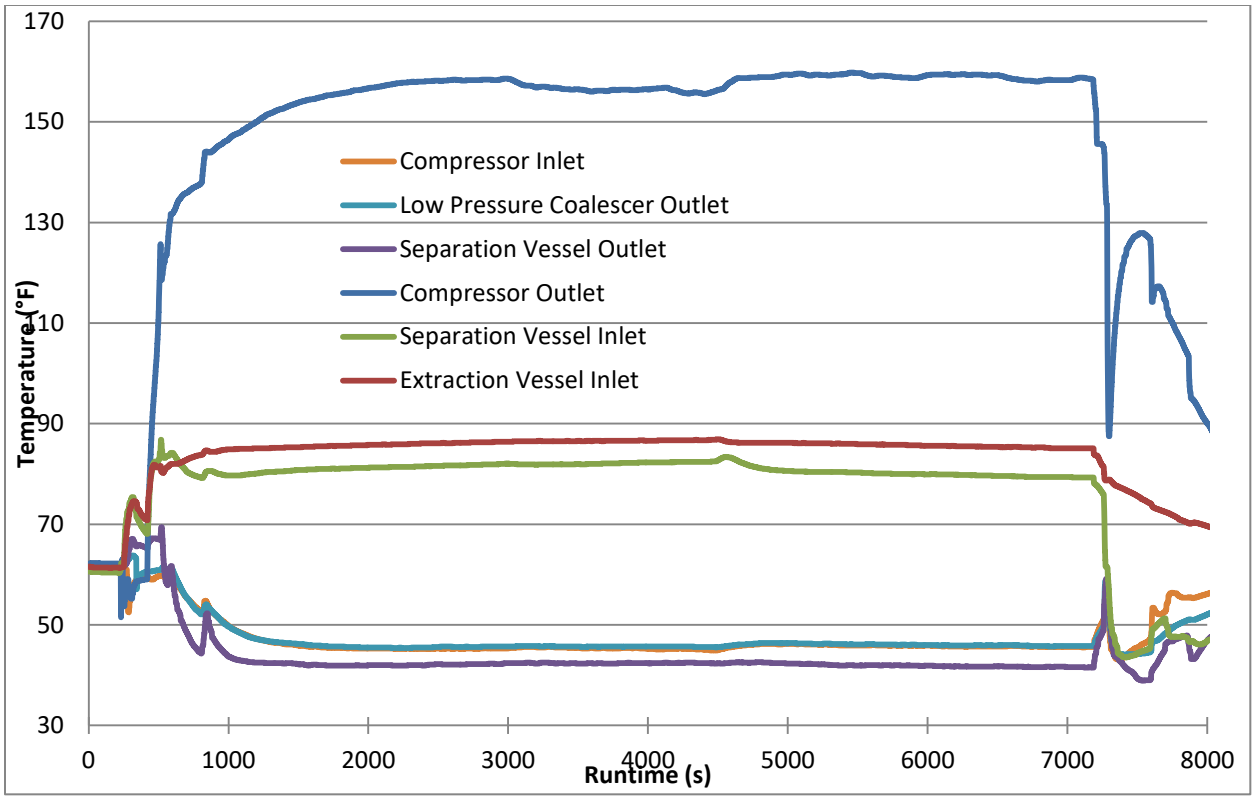

Figure 37: Run 3 Temperature Plot

Figure 37 is a plot of the recorded system operating temperatures over run 3 of the system. The plot for run three shows the most successful steady state run out of all three system runs which took place. The initial starting point can be seen on the left side of the plot with initial starting temperatures of around 60 °F. The temperature of the compressor outlet quickly rises. The plot of the compressor outlet temperature in blue shows a smooth temperature differential throughout the operation of run 3, staying relatively constant at 157 °F. This constant operation of the compressor sharply contrasts that of run 2 where the compressor continuously cycled between significantly lower temperatures. The thermal image of the three way valve after the compressor where temperature of the compressor outlet was taken can be seen in Figure 38.

Figure 38: High Pressure 3-way Valve, Compressor Outlet Temperature

The low pressure side of the system can be seen in Figure 37 by the plots of the compressor inlet, low pressure coalescer outlet and the separation vessel outlet temperatures which are all constant throughout run 3. The constant temperature on the low side is the optimal operation which had not occurred in the two previous runs. This steady state operation in run 3 does not show any sign of temperature creep as in the previous two runs. The silicone heater tape continued to be implemented on the low pressure separation vessel however both a thermocouple and watt meter were incorporated in order track and monitor the amount of heat entering the system. A thermal image of the silicone heater tape on the low pressure separation vessel can be seen in the Figure 39.

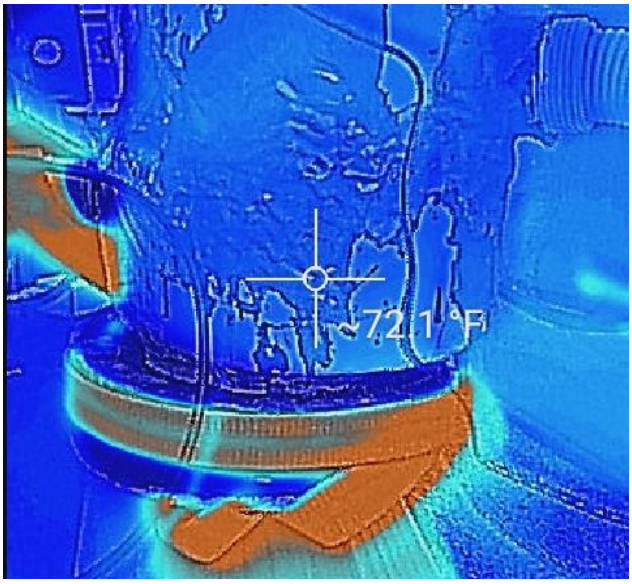

Figure 39: Heat Tape & Low Pressure Separation Vessel

Not only were steady state temperatures seen in the CO_2 throughout the system, they were also seen in the heat exchanger water loop shown in the Figure 40.

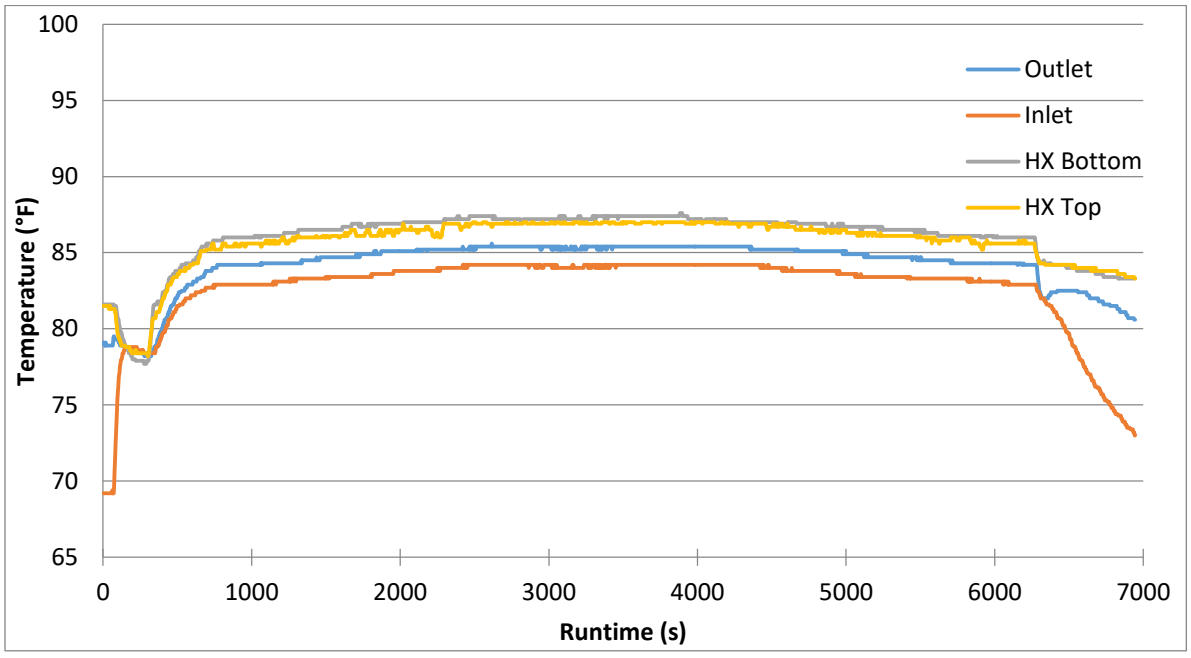

Figure 40: Run 3 Heat Exchanger Temperatures

From this plot of the heat exchanger temperature we can clearly see the rise in temperature from the start of operation however temperatures begin to level off and reach

a steady state point within the first 20 minutes of operation. This data shows a 1.1 °F temperature difference between the inlet and outlet temperature and using the measured flowrate of 4 GPM, the average heat exchange rate of 2,200 BTU/hr was determined.

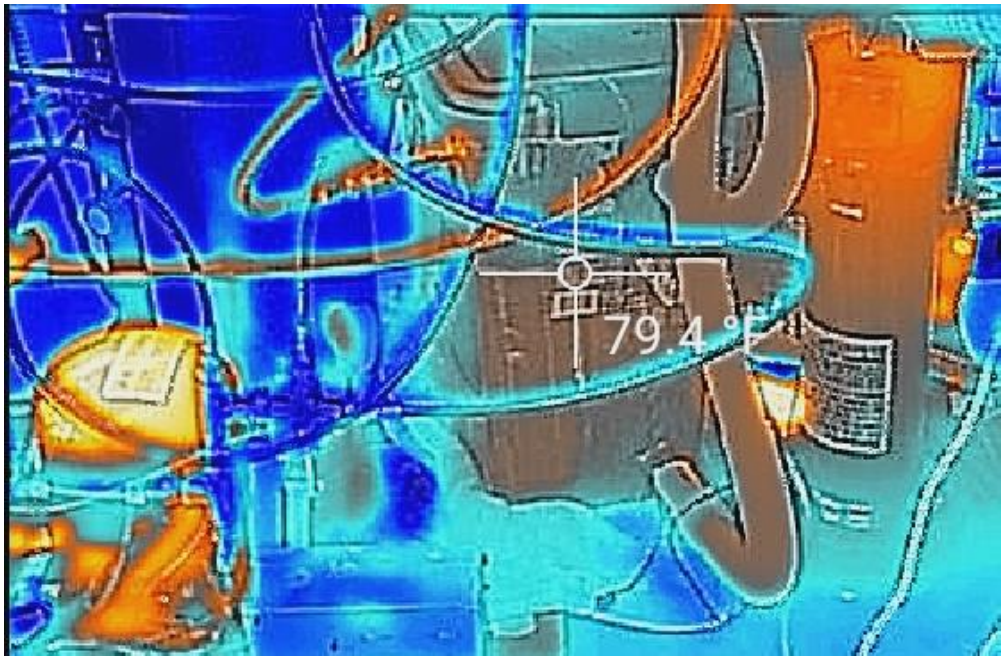

Figure 41: Thermal Image of Run 3 System at Steady State

In the Figure 41, the temperature distribution can be seen in the supercritical extraction vessel on the right of the image. The temperature distribution is evident based on the difference in orange color between the top and bottom of the vessel. It is also noticeably cooler than the thermal image of the extraction vessel during run 2. As a result of achieving stead state operating temperatures in the system, the plot of temperatures after the gas cooler and inside of the supercritical extraction vessel show no signs of temperature creep. The plotted temperatures of the separation vessel inlet and the extraction vessel inlet in Figure 37 show the constant temperature of the supercritical fluid after the gas cooler throughout the period of operation.

Based on the pressure and temperature operating conditions from the start of operation until the end of operation, the density of the supercritical CO_2 after the gas

cooler and in the extraction vessel begins at 47 lb/ft^3 and decreases slightly in density until reaching 45.6 lb/ft^3 by the end of the third run. Due to the relatively low temperature of the supercritical fluid after the gas cooler and in extraction chamber the coffee beans experienced relatively constant extraction by a supercritical CO_2 fluid which was 75% as dense as water at room temperature.

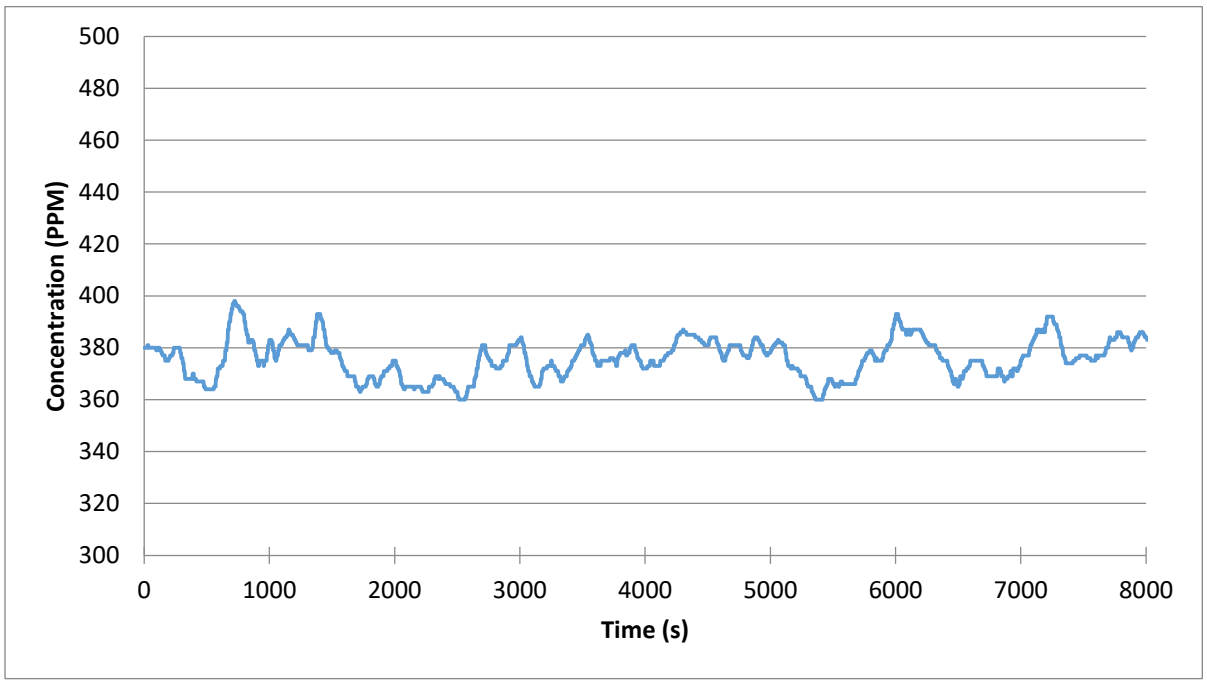

Figure 42: Run 3 CO_2 Concentrations

Figure 42 shows CO_2 levels in PPM throughout the duration of the third run. As seen in the figure, throughout operation the CO_2 in the operating environment was within normal safe levels at around 380 ppm. There are small spikes in CO_2 concentration throughout the run time of the unit however due to the fact that the fluctuation is within a 20 ppm range, this could be due to exterior environmental changes or error in the CO_2 monitoring devise.

Chapter 5: Conclusion

The goal of this thesis was to explore the potential of using Supercritical CO_2 as a solvent and testing the ability to build a low budget apparatus for the use of extracting caffeine from coffee beans. This goal was accomplished through the implementation of three test runs. After the initial system design and build the system was tested and determined to be leak free. This system was then proven to be safe to operate by running pressure tests over increasing periods of time. Finally the system was proven to be operational by the more than seven hours of supercritical CO_2 testing time which it preformed.

Throughout this project the system design was proven to be both functional and safe. The first operational run of the unit was completed without coffee beans in order to test the function of the system in a shake-down experiment. The second run was also used as a shake-down experiment to test the ability of the system to operate with a substance inside of the supercritical vessel. The third run was successful in the extraction of caffeine from the roasted coffee beans with an extraction efficacy estimated to be between 5 and 10 percent, showing that a small-scale supercritical CO_2 extraction apparatus implementing CO_2 as a green solvent was feasible. Given the opportunity to build another supercritical CO_2 extraction apparatus with a larger operating budget, there would be a few design modifications.

First, given the ability, it would be optimal to implement an oil-free diaphragm compressor, which is designed to be used in supercritical CO_2 extraction systems like this. Due to the fact that this thesis was student funded, this $30,000 piece of equipment was unfortunately not accessible. The ability to implement an oil-free diaphragm compressor would allow for further supercritical testing without having to worry about oil, particulates, moisture or anything else that could enter the compressor and result in

damage overtime. Furthermore, given the opportunity to rebuild the prototype a transcritical refrigeration compressor with a recirculating oil pump could also be tested. Although this would not be the preferable option, due to the oil circulation it could also be implemented in this design.

Given the ability to use an oil-free diaphragm compressor, the other major design change would be in both the extraction vessel as well as the separation vessel. Since the diaphragm compressor is the driving force for the flow through the system, the supercritical extraction vessel could be increased in volume by up to five times. This increase in extraction vessel volume would allow the ability to extract from a large volume of coffee beans per extraction run. Since the size of the extraction vessel is only limited by the size of the systems CO_2 tank reservoir, the current 50lb tank would be capable of meeting the system's charging demands. Given the implementation of a larger extraction vessel, the separation vessel could remain the same size as in this current apparatus since the extracted caffeine from the coffee beans would only be one percent of the original weight in the extraction vessel at maximum.

The next major design change that would be made would involve the heat exchanger water system. Instead of attempting to transfer the heat from the high side after the compressor in order to provide the load for the low pressure side flash tank after the expansion devise, this process would be removed completely. The design would be similar to that of any refrigeration system where the excess heat from the compressor would simply be discharged through air cooled fins into the surrounding environment. In order to provide enough heat load for the low pressure side, a properly sized heating element would be applied to the outside of the low pressure expansion vessel to balance the load so that the system could operate at steady state. This would allow the system the flexibility to cool the high side temperature after the compressor to roughly 15 degrees

above ambient conditions. Given this as a baseline for operation, an ice chest or secondary cooling system could be implemented for testing supercritical extractions at lower fluid temperature and higher densities.

This project culminated in the extraction of one gram of caffeine and coffee oils, and through the research, design, build and experiment process a significant amount of data was gained. Through this data the feasibility of using supercritical CO_2 in a small-scale system was shown and recommendations for future system designs were determined.

BIBLIOGRAPHY

Caffeine in Coffee (2015, April 23). In Brew Your Mind. Retrieved February 25, 2017, from https://www.coffeechemistry.com/chemistry/alkaloids/caffeine-in-coffee

Gupta, Ram B., and Shim. *Solubility in supercritical carbon dioxide*. Boca Raton: CRC Press, 2007. Print.

Leitner, Walter, et al. *Green solvents*. Weinheim: Wiley-VCH, 2010. Print.

McHugh, Mark A., and Val J. Krukonis. *Supercritical fluid extraction: principles and practice*. Boston: Butterworth-Heinemann, 1994. Print.

Mukhopadhayay, Mamata. *Natural Extracts Using Supercritical Carbon Dioxide*. Boca Raton, CRC Press LLC, 2000.

Taylor, Larry T. *Supercritical Fluid Extraction*. New York, John Wiley & Sons, Inc., 1996.

Thurman, E. M., and M. S. Mills. *Solid-phase extraction: principles and practice*. New York: Wiley, 1998. Print.

APPENDICES

Appendix A: Bill of Materials

Table 15: Detailed Bill of Materials for System

Item	#	$	Total	Website
pressure gauge	8	62	496	https://www.aliexpress.com/item/0-60Mpa-8700psi-G1-4-0-25-Accuracy-Battery-Powered-Digital-Pressure-Gauge/1949156287.html
Quick Connects	18	4	72	
Thermocouple	8	40	320	http://www.omega.com/pptst/TC-NPT.html
Flow Meter	1	60	60	http://www.ebay.com/itm/201631479381?_trksid=p2057872.m2749.l2649&ssPageName=STRK%3AMEBIDX%3AIT
3 way valve	2	50	100	http://www.ebay.com/itm/152047082514?_trksid=p2057872.m2749.l2649&ssPageName=STRK%3AMEBIDX%3AIT
2 way valve	8	20	160	http://www.ebay.com/itm/1-4-High-Pressure-Steel-Ball-Valve-7250-PSI-NPT-Full-Port-2-WAY-/162032267059?hash=item25b9e02f33
Diaphragm Valve	2	110	220	http://www.ebay.com/itm/Swagelok-SS-DSTF4-1-4-FNPT-Diaphragm-Valve-Stainless-Steel-/121052310734?hash=item1c2f47acce
8 channel data logger	1	100	100	http://www.ebay.com/itm/8-Channel-Temperature-Data-Logger-V2-Arduino-DS18B20-55-125C-Thermometer-/111945784330?hash=item1a107d1c0a
4 channel Temp logger	2	150	300	https://www.amazon.com/gp/product/B01HD4WMS8/ref=oh_aui_detailpage_o04_s00?ie=UTF8&psc=1
Burst Disc	1	20	20	
Scale	1	30	30	https://www.amazon.com/gp/product/B00I9D5IFM/ref=oh_aui_detailpage_o03_s01?ie=UTF8&psc=1
CO_2 Tank	1	250	250	
Sanden System	1	450	450	
Cart	1	100	100	
Hoses	10	10	100	
Total			$2,778	

Appendix B: Calculations & EES Code

```
$REFERENCE R744 ASH

"Critical State Values"
r$ = 'R744'                                          "Carbon Dioxide Refrigerant"
PC = P_crit(r$)                                      "Critical Pressure"
TC = T_crit(r$)                                      "Critical Temp"
m_dot = 30                                           "CO2 Mass Flow"
T_amb = 60 [F]                                       "Temp Ambient"
T_app = 20 [F]                                       "Temp Approach"
"State 1"
P[1] = 400                                           "Compressor Inlet Pressure"
H[1] = Enthalpy(r$,T=T[1],P=P[1])                    "Enthalpy State 1"
S[1] = Entropy(r$,T=T[1], P=P[1])                    "Entropy State 1"
T[1] = Temperature(r$,P=P[1],H=H[1])                 "Compressor Inlet Temp"
"State 2/ Compressor"
P[2] = 1300                                          "Compressor Outlet Pressure"
eta_c = .95                                          "Compressor Efficiency Calc"
H_2 = Enthalpy(r$,P=P[2],S = S[1])                   "Enthalpy State 3 Isentropic"
Q_dot_compressor = m_dot*((H[2]-H[4])-(H[1]-H[5]))   "Compressor Heat Rejection"
T[2] = Temperature(r$,P=P[2],H=H[2])                 "Temp Compressor outlet"
H[2] = (H_2-H[1])/eta_c + H[1]                       "Enthalpy State 2"
S[2] = Entropy(r$,T=T[2], P=P[2])                    "Entropy State 2"
Q_hi = (m_dot*(H[2]-H[3])) - Q_dot_compressor        "Heat Rejection Gas Cooler"
"State 3"
H[3] = Enthalpy(r$,T=T[3],P=P[3])                    "Enthalpy State 3"
S[3] = Entropy(r$,T=T[3], P=P[3])                    "Entropy State 3"
T[3] = T[4] + 5                                      "Temp State 3"
P[3] = P[2]                                          "Pressure State 3"
"State 4"
P[4] = P[3]                                          "Pressure State 4"
T_4 = T_amb + T_app                                  "Temp Extraction Vessel"
T[4] = T_4                                           "Temp State 4"
H[4] = Enthalpy(r$,P=P[3],T=T[4])                    "Enthalpy State 4"
S[4] = Entropy(r$,T=T[4],P=P[3])                     "Entropy State 4"
"State 5"                                            "Low Side Expansion Valve"
P[5] = P[1]                                          "Pressure State 5, After
Expansion"
H[5] = H[4]                                          "Enthalpy State 5"
X[5] = Quality(r$,P=P[5],H=H[5])                     "Quality State 5"
T[5] = Temperature(r$,P = P[5], H = H[5])            "Temp Separation Vessel"
S[5] = Entropy(r$,P=P[5],H= H[5])                    "Entropy State 5"
"State 6"
P[6] = P[1]                                          "Pressure State 6"
H[6] = H[1]                                          "Enthalpy State 6"
S[6] = Entropy(r$,T=T[6],P=P[6])                     "Entropy State 6"
T[6] = Temperature(r$,P = P[6], H = H[6])            "Temp State 6"
```

Table 16: Volume Calculations

Part	Liters	Liters Total	Volume (m)	OD (in)	ID (in)	#	Length (in)	Length Total (in)	Area (in^2)	Volume (in^3)
Pressure Vessels	2.31	4.62	0.00462			2				281.93
Oil Filter	0.31	0.62	0.00062			2				37.83
Gas Cooler				0.2	0.1	47	13	611	0.0079	4.80
Compressor					5.5		6	0.3	285.1	75.53
Additional Pipe				0.315	0.157			250	0.02	4.87
									Total Volume	**404.96**

Table 17: Preliminary CO_2 Charge Estimation Calculations

						Charge	
T (F)	**P (psi)**	**Part**	**Density (kg/m^3)**	**Volume (in^3)**	**Volume CO_2 (m^3)**	**CO_2 (Kg)**	**CO_2 (lbs)**
150	1500	**Comp > G.C.**	290	90	1.47E-03	0.43	0.94
90	1500	**G.C. > Low P**	746	155	2.54E-03	1.89	4.18
66	809	**Low P. liquid 25%**	785	37.5	6.15E-04	0.48	1.06
70	809	**Low P > Comp**	157	150	2.46E-03	0.39	0.85
		Total System Charge					**7.033**